1997-03-01

Upf1p, Nmd2p, and Upf3p are interacting components of the yeast nonsense-mediated mRNA decay pathway

Feng He
University of Massachusetts Medical School

Et al.

MOLECULAR AND CELLULAR BIOLOGY, Mar. 1997, p. 1580–1594 Vol. 17, No. 3
0270-7306/97/$04.00+0

Upf1p, Nmd2p, and Upf3p Are Interacting Components of the Yeast Nonsense-Mediated mRNA Decay Pathway

FENG HE, AGNETA H. BROWN, AND ALLAN JACOBSON*

Department of Molecular Genetics and Microbiology, University of Massachusetts Medical School, Worcester, Massachusetts 01655-0122

Received 7 October 1996/Returned for modification 1 November 1996/Accepted 22 November 1996

Rapid turnover of nonsense-containing mRNAs in *Saccharomyces cerevisiae* is dependent on Upf1p, Nmd2p, and Upf3p, the products of the *UPF1*, *NMD2*/*UPF2*, and *UPF3* genes, respectively. We showed previously that Upf1p and Nmd2p interact and that this interaction is required for nonsense-mediated mRNA decay (F. He and A. Jacobson, Genes Dev. 9:437–454, 1995; F. He, A. H. Brown, and A. Jacobson, RNA 2:153–170, 1996). In this study we have used the yeast two-hybrid system to define other protein-protein interactions among the essential components of this decay pathway. Nmd2p-Upf3p and Upf1p-Upf3p interactions were identified, and the respective domains involved in these interactions were delineated by deletion analysis. The domains of Upf1p and Upf3p putatively involved in their mutual interaction were found to correspond to the domains on the two proteins which interact with Nmd2p, suggesting that Nmd2p bridges Upf1p and Upf3p. This conclusion was reinforced by experiments showing that: (i) deletion of *NMD2* completely abolishes interactions between Upf1p and Upf3p and (ii) overexpression of full-length Nmd2p or Nmd2p fragments that retain Upf1p- and Upf3p-interacting domains promotes 10- to 200-fold enhancement of Upf1p-Nmd2p-Upf3p complex formation. These results; the observation that cells harboring either single or multiple deletions of *UPF1*, *NMD2*, and *UPF3* inhibit nonsense-mediated mRNA decay to the same extent; and an analysis of the possible targets of a dominant-negative *NMD2* allele indicate that Upf1p, Nmd2p, Upf3p, and at least one other factor are functionally dependent, interacting components of the yeast nonsense-mediated mRNA decay pathway.

Decay of eukaryotic mRNAs can be triggered by poly(A) shortening, endonucleolytic cleavage, or aberrant translation (for a review, see reference 16). Aberrant translation includes nonsense-mediated mRNA decay, the rapid turnover of an otherwise stable mRNA that ensues when a ribosome encounters a premature translational termination codon. This phenomenon has been observed in both prokaryotic and eukaryotic cells but has been best characterized for *Saccharomyces cerevisiae* (for reviews, see references 16 and 27). In the yeast system this type of mRNA decay is cytoplasmic and depends on, in addition to a nonsense codon, at least two *cis*-acting coding-region sequences and several *trans*-acting factors (27). The coding-region sequences include a site 3′ to the nonsense codon that appears to promote translational reinitiation and messenger ribonucleoprotein (mRNP) conformational changes and a sequence that, when translated, inactivates a ribosome's capacity to promote rapid mRNA decay (10a, 16, 25, 40).

trans-acting factors required for nonsense-mediated mRNA decay were initially identified by a genetic screen for allosuppressors of the *his4-38* frameshift allele (6). Subsequent screens that also identified components of this pathway included those seeking mutations that increased frameshifting efficiencies (8, 20), suppressors of upstream initiation codons (28), and omnipotent suppressors (41). Complementation of these mutants, or the use of two-hybrid screens, led to the isolation of the nonessential *UPF1* (*IFS2*/*SAL2*/*MOF4*), *NMD2* (*UPF2*/*SUA1*/*IFS1*), and *UPF3* (*SUA6*) genes and to the demonstration that mutations in these genes cause stabilization and increased accumulation of nonsense-containing mRNAs while having no effect on the stabilities or abundances of most wild-type transcripts (5, 12, 13, 19–21, 25).

* Corresponding author. Phone: (508) 856 2442. Fax: (508) 856 5920. E-mail: ajacob@ummed.edu.

Of the *trans*-acting factors identified by these approaches, that encoded by the *UPF1* gene has been studied most extensively. The *UPF1* gene encodes a protein that has a predicted molecular mass of 109 kDa, two putative Zn^{2+} fingers near its N terminus, and seven conserved motifs common to the members of helicase superfamily I (1, 18, 22). Upf1p is localized primarily in the cytoplasm and appears to be polyribosome associated (3, 26). Upf1p has recently been purified from yeast cells and shown to possess nucleic acid-binding activity as well as nucleic acid-dependent ATPase and helicase activities (7). Characterization of the *NMD2* gene indicates that it encodes an acidic protein with a predicted molecular mass of 127 kDa and no significant homologies to other polypeptides (5, 12). Two-hybrid analyses demonstrate that Nmd2p and Upf1p are interacting proteins and that the Upf1p-interacting domain of Nmd2p is localized within a 157-amino-acid segment at its C terminus (14). Mutations in this domain that disrupt interaction with Upf1p also inactivate nonsense-mediated mRNA decay, indicating that Upf1p-Nmd2p interaction is required for function of this decay pathway (14). The *UPF3* gene encodes a basic protein with a predicted molecular mass of 45 kDa (19). Upf3p has no significant homologies to other proteins, but, like Nmd2p (12), Upf3p contains multiple lysine-arginine-rich sequences that resemble bipartite nuclear localization sequences known to target proteins to the nucleus (19).

Although the identification and initial characterization of Upf1p, Nmd2p, and Upf3p have provided insight into the mechanism of nonsense-mediated mRNA decay, the precise functions and interactions of these factors are largely unknown. Given that single disruptions of *UPF1*, *NMD2*, and *UPF3* inhibit nonsense-mediated mRNA decay to the same extent, and that double disruptions are not additive, it appears that Upf1p, Nmd2p, and Upf3p may function as a complex or in closely related steps of this mRNA decay pathway (5, 12, 19, 37). Except for the interaction between Upf1p and Nmd2p (12,

14), interactions between these factors have not been characterized extensively. To address this problem, we have used the yeast two-hybrid system to identify genes encoding Nmd2p-interacting proteins, to characterize the specific domains involved in Upf1p-Nmd2p and Nmd2p-Upf3p interactions, and to show that Nmd2p can interact with both Upf1p and Upf3p simultaneously, possibly promoting the formation of a Upf1p-Nmd2p-Upf3p complex in vivo. Our two-hybrid studies and the analysis of mRNA decay in strains with one or more of these factors deleted as well as in strains harboring a dominant-negative *NMD2* allele lead us to conclude that Upf1p, Nmd2p, Upf3p, and at least one other factor are interacting components of the nonsense-mediated mRNA decay pathway.

MATERIALS AND METHODS

General methods. Preparation of standard yeast media and methods of cell culture were as described previously (30). Transformation of yeast was done by the high-efficiency method (34), and DNA manipulations were performed by standard techniques (32). All PCR amplifications were performed with *Taq* DNA polymerase (38) and confirmed, when appropriate, by DNA sequencing according to the method of Sanger et al. (33). Plasmid DNAs were prepared from *Escherichia coli* DH5α.

Oligonucleotides. The oligonucleotides used in this study were obtained from Operon, Inc., and are listed in Table 1.

Yeast strains. The yeast strains used in this study are listed in Table 2. The two-hybrid tester strains containing deletions of *UPF1*, *NMD2*, and *UPF3* were constructed by gene replacement (31). HFY869, harboring a deletion of the *UPF1* gene, was constructed by transforming the L40 strain with a *Not*I-*Sal*I fragment from Bs-*upf1::HIS3* (pHF1395) (Table 3). HFY863, harboring a deletion of the *NMD2* gene, was constructed by transforming the L40 strain with a *Not*I-*Sal*I fragment from Bs-*nmd2::HIS3* (12). HFY866, harboring a deletion of the *UPF3* gene, was constructed by transforming the L40 strain with a *Not*I-*Sal*I fragment from Bs-*upf3::HIS3* (pHF1409) (Table 3). In each case, His^+ transformants were selected, the disruption event was confirmed by PCR analysis, and the inactivation of nonsense-mediated mRNA decay was monitored by Northern blot analysis with *CYH2* as a probe. The yeast strains HFY870 and HFY861, harboring deletions of the *UPF1* and *UPF3* genes, respectively, were constructed in the same way as the HFY869 and HF866 strains except that strain HFY1200 was used for transformations. HFY872, harboring deletions of both the *UPF1* and *UPF3* genes, was constructed by transforming HFY861 with a *Not*I-*Sal*I fragment from Bs-*upf1-1::URA3* (pHF1397) (Table 3). HFY874, harboring deletions of both the *NMD2* and *UPF3* genes, was constructed by transforming HFY861 with a *Not*I-*Sal*I fragment from Bs-*nmd2::URA3* (pHF275) (Table 3). HFY883, harboring a triple deletion of the *UPF1*, *NMD2*, and *UPF3* genes, was constructed by transforming HFY874 with a *Bam*HI-*Xho*I fragment from pRS314-*upf1::LEU2* (see below). For each construction, the disruption event was confirmed by PCR analysis.

Plasmid constructions. The plasmids used in this study included (i) the *GAL4* activation domain [*GAL4*(AD)]-containing plasmids pACTII (a generous gift from Stephen Elledge, University of Texas, Houston), pGAD-C1, pGAD-C2, and pGAD-C3 and plasmid libraries containing yeast genomic DNA fused to the *GAL4*(AD) (generous gifts from Philip James and Elizabeth Craig, University of Wisconsin Medical School, Madison, and David Mangus, University of Massachusetts Medical School, Worcester); (ii) the *GAL4* and *lexA* DNA-binding domain [*GAL4*(DB) and *lexA*(DB)]-containing plasmids pMA424 and pBTM116 (generous gifts from Stanley Fields, University of Washington, Seattle, and Stanley Hollenberg, Fred Hutchinson Cancer Research Center, Seattle, respectively); (iii) pRS314-*upf1::LEU2*, a *UPF1* deletion-disruption plasmid (a generous gift from Aidan Hennigan); (iv) pRS313, pRS314, and pRS316, yeast shuttle plasmids containing ARS4 and CEN6 and the *HIS3* gene (pRS313), the *TRP1* gene (pRS314), or the *URA3* gene (pRS316) gene (35); (v) YEplac112, a yeast 2μm vector containing the *TRP1* gene (11); (vi) Bluescript KS(+), an *E. coli* cloning vector (Stratagene); (vii) Bs-*nmd2::HIS3*, pRS315-*NMD2*(X-S), pRS315-HA-*NMD2*(X-S), pRS316-HA-*NMD2*(X-S), pRS315-HA-*nmd2-CΔ166*, YEplac112-*NMD2*(X-S), YEplac112-HA-*NMD2*(X-S), pHF926, pACTII-*NMD2-CΔ166*, and pACTII-$NMD2^{DN}$, the construction of which was described previously (12, 14); and (viii) the set of plasmids whose features are summarized in Tables 3 and 4 and whose construction is outlined below.

(i) *GAL4*(AD)-*UPF1* fusion constructs. All *GAL4*(AD)-*UPF1* fusions used for mapping the Nmd2p- and Upf3p-interacting domains of Upf1p were constructed by using PCR-derived fragments. In each case, a pair of oligonucleotide primers containing either an *Eco*RI site (5′ primer) or a *Sal*I site (3′ primer) was used for amplification (Table 1). The PCR-amplified fragment was digested with *Eco*RI and *Sal*I and ligated into pACTII* digested previously with *Eco*RI and *Xho*I. The resulting plasmids each carried a distinct fragment from the *UPF1* coding region (Table 4). The plasmid pACTII* is a modified version of pACTII (9) and was constructed by ligating an *Eco*RI linker (GGAATTCC) into pACTII digested previously with *Sma*I. This led to a change from GCC CCG GGG to GCC CCG GAA TCC GGG, in which the *Eco*RI site is in the same reading frame as that of pMA424, pBTM116, and pGAD-C1, pGAD-C2, and pGAD-C3.

(ii) *lexA*(DB)-*NMD2* fusion constructs. The plasmid pHF1186 (Table 4) was used for the two-hybrid screen. It carries a *lexA*(DB)-$NMD2^{DN}$(326–1089) fusion and was constructed as follows. A 210-bp PCR-derived *Eco*RI-*Cla*I fragment (from codon 326 to the *Cla*I site in the *NMD2* coding region) was ligated into Bluescript KS(+) digested previously with *Eco*RI and *Cla*I. The resulting plasmid, pHF1201 (Table 3), was then digested with *Cla*I and *Sal*I and ligated to a 3.5-kb *Cla*I-*Sal*I *NMD2* fragment isolated from pRS316-HA-*NMD2*(X-S) (14), creating pHF1203. A 5′-end 1,339-bp *Eco*RI-*Pst*I fragment and a 3′-end 2.4-kb *Pst*I-*Sal*I fragment were individually isolated from pHF1203 and were ligated into pBTM116 digested previously with *Eco*RI and *Sal*I in a three-fragment ligation reaction.

The plasmid pHF1268, which carries a *lexA*(DB)-*NMD2* fusion containing an N-terminal deletion up to residue 772, was constructed by ligating a 2.3-kb *Eco*RI-*Sal*I fragment isolated from pHF1186 into pBTM116 digested previously with *Eco*RI and *Sal*I. The plasmids pHF1308, pHF1309, pHF1311, and pHF1313, which carry *lexA*(DB)-*NMD2* fusions containing N-terminal deletions up to residues 473, 564, 638, and 693, respectively, were constructed by using pHF1268. In each case, a pair of oligonucleotide primers containing either *Eco*RI/*Bam*HI sites (5′ primer) or an *Eco*RI site (3′ primer, *NMD2*-M11) were used for amplification (Table 1) (14). The PCR-amplified fragment was digested with *Eco*RI and ligated into pHF1268 digested previously with *Eco*RI. The correct orientation of each insert was confirmed by restriction digestion. The plasmids pHF1304 and pHF1306, which carry *lexA*(DB)-*NMD2* fusions containing N-terminal deletions up to residues 817 and 879, respectively, were constructed by using PCR-derived fragments. The oligonucleotide primer pairs *NMD2*-TH29/*NMD2*-M10 and *NMD2*-TH30/*NMD2*-M10 were used for amplification (Table 1) (14). The PCR-amplified fragments were digested with *Eco*RI and *Sal*I and ligated individually into pBTM116 digested previously with *Eco*RI and *Sal*I. Plasmid pHF1270, which carries a *lexA*(DB)-*NMD2* fusion containing an N-terminal deletion up to residue 933, was constructed by ligating the 1.1-kb *Eco*RI-*Sal*I fragment isolated from pHF1050 (see below) into pBTM116 digested previously with *Eco*RI and *Sal*I.

The plasmids pHF1262, pHF1264, pHF1266, pHF1352, pHF1349, pHF1348, pHF1345, and pHF1344 carry *lexA*(DB)-*NMD2* fusions with distinct C-terminal deletions and were constructed by using pHF1186. In each case, a *Cla*I-*Sal*I fragment from the C-terminal region of the individual HA-*nmd2* alleles that harbor distinct C-terminal deletions (see below and Table 3) was isolated and ligated into pHF1186 digested previously with *Cla*I and *Sal*I. The plasmids pHF1467, pHF1469, pHF1471, and pHF1473 carry *lexA*(DB)-*NMD2*(564–923), *lexA*(DB)-*NMD2*(564–883), *lexA*(DB)-*NMD2*(564–816), and *lexA*(DB)-*NMD2*(564–803) fusions, respectively. They were constructed by ligating a 630-bp *Eco*RI-*Eco*RI fragment (from codon 564 to the *Eco*RI site in the coding region of pHF1309-borne *NMD2*) into pHF1262, pHF1264, pHF1266, and pHF1352 digested previously with *Eco*RI. The plasmids pHF1528 and pHF1530, which carry *lexA*(DB)-*NMD2*(564–771) and *lexA*(DB)-*NMD2*(564–692) fusions, respectively, were constructed by the following three-fragment ligations: a PCR-amplified *Eco*RI-*Bgl*II fragment and a 0.6-kb *Bgl*II-*Sal*I fragment isolated from pHF926 were ligated into pBTM116 digested previously with *Eco*RI and *Sal*I. The oligonucleotide pairs *NMD2*-TH25/*NMD2*-TH31 and *NMD2*-TH25/*NMD2*-TH32 (Table 1) were used for amplification of the respective fragments.

(iii) *GAL4*(DB)-*NMD2* and *GAL4*(AD)-*NMD2* fusion constructs. The plasmid pHF1050, which carries the *GAL4*(DB)-*NMD2*(933–1089) fusion, was used for mapping the Nmd2p-interacting domain of Upf1p. It was constructed by ligating a PCR-amplified *Eco*RI-*Sal*I fragment into pMA424 digested previously with *Eco*RI and *Sal*I. The oligonucleotides *NMD2*-TH18 and *NMD2*-M10 were used for PCR amplification (Table 1) (14).

The plasmids pHF1415, pHF1417, pHF1419, pHF1421, pHF1425, and pHF1427, which carry *GAL4*(AD)-*NMD2* fusions containing N-terminal deletions up to residues 473, 564, 638, 693, 817, and 879, respectively, and the plasmids pHF1670, pHF1672, pHF1674, pHF1676, pHF1534, and pHF1536, which carry *GAL4*(AD)-*NMD2* fusions each containing an internal fragment beginning at codon 564, were constructed in the same way. In each case, a *Bam*HI-*Sal*I fragment was isolated from the corresponding *lexA*(DB)-*NMD2* fusion plasmid (Table 4) and ligated into pGAD-C1 digested previously with *Bam*HI and *Sal*I. The plasmid pHF1423, which carries the *GAL4*(AD)-*NMD2*(772–1089) fusion, was constructed by ligating a PCR-amplified *Bam*HI-*Sal*I fragment into pGAD-C1 digested previously with *Bam*HI and *Sal*I. The oligonucleotides *NMD2*-TH28 and *NMD2*-M10 were used for PCR amplification. The plasmids pHF1429 and pHF1431, which carry the *GAL4*(AD)-*NMD2*(933–1089) and *GAL4*(AD)-*NMD2*(326–563) fusions, respectively, were constructed by ligating *Eco*RI-*Sal*I fragments isolated from pHF1050 and pHF1344, respectively, into pGAD-C1 digested previously with *Eco*RI and *Sal*I. The plasmid pHF1441, which carries a *GAL4*(AD)-*NMD2* fusion with the original dominant-negative fragment encoding Nmd2p residues 326 to 1089 (12), and the plasmids pHF1458, pHF1456, pHF1454, pHF1452, pHF1450, pHF1448, and pHF1446, which carry *GAL4*(AD)-*NMD2* fusions each containing a distinct C-terminal deletion, were constructed by using pHF1431. In each case, a *Cla*I-*Sal*I fragment from the C-terminal regions of the individual HA-*nmd2* alleles, each harboring a distinct C-terminal deletion (Table 3), was isolated and ligated into pHF1431 digested previously with *Cla*I and *Sal*I.

TABLE 1. Oligonucleotides

Name	Sequence (5′ to 3′)
UPF1-TH1	CCGGAATTCATGGTCGGTTCCGGTTCT
UPF1-TH2	CCGGAATTCTGTGCGTATTGTGGTATAGATTCT
UPF1-TH3	CCGGAATTCGATACCGTTTTGGAATGTTATAAC
UPF1-TH4	CCGGAATTCGAGTTGAAAGTTGCCATCGGTGAT
UPF1-TH3-2	ACGCGTCGACTTATATTCCCAAATTGCTGAAGTC
UPF1-TH6	ACGCGTCGACTTAGGATCTCCATTTTGCCTCCAACTT
UPF1-TH7	ACGCGTCGACTTAGTTAGATTCGAAAGTAGATAAAGT
UPF1-TH10	CCGGAATTCGGTGCTGGTGATAAGCGCTTA
UPF1-TH13	CGCGTCGACTTATACATGACTAACAGCGTTCGA
UPF1-TH14	CGCGTCGACTTAAACACATGTGCAACATACGAC
UPF1-TH15	CGCGTCGACTTAACGCTGTTCAATCGTTACACC
UPF1-TH16	CGCGTCGACTTATTGCTCTGCGACCCATGATAA
UPF1-TH17	CGCGTCGACTTAGGCACAAGGTATTCTACAAAG
UPF1-DS1	ACAGAATTCATGAACGGGAAATAAGAA
UPF1-DS2	CGAAGATCTTTGATAATGACAATGATTGATGTA
UPF1-DS3	CGAAGATCTATCGATTTCGGTGAACCCTGTTAAAATAAA
UPF1-DS4	CGCGTCGACTATTATCTGTGGTATCATTTTCTA
NMD2-TH18	CCGGAATTCAGCGACTCTGATTTGGAGTATGGT
NMD2-TH21	CCGGAATTCATCACGAATCAGATATTGCCACCC
NMD2-TH22	CGCAGATCTCAACTTTTTATTGCGTTTAATGAT
NMD2-TH23	CGCAGATCTCATTGCTTTGCCTGATGTTTTCCT
NMD2-TH24	ACAGAATTCGGATCCAGTGAAATGATTAAATTTCAA
NMD2-TH25	ACAGAATTCGGATCCAAATCATTAAATGTTACGGTA
NMD2-TH26	ACAGAATTCGGATCCGGTCTATACAGTTACCGCCGC
NMD2-TH27	ACAGAATTCGGATCCGTTTTGTTAGATACTATCTAC
NMD2-TH28	CGCGGATCCGAATTCAGAGTTTCAAGCACATTT
NMD2-TH29	ACAGAATTCGGATCCAAAGACGACAGAGTGAAGGGA
NMD2-TH30	ACAGAATTCGGATCCCATCAGGCAAAGCAAGACGAA
NMD2-TH31	ACGCAGATCTCATGTTTCCTTGGGTAAAGGTTG
NMD2-TH32	ACGCAGATCTCAATCGGATTTTATCATTTCAAA
NMD2-TH33	ACGCAGATCTCAGCCTAGAACTTTTGTTAATAA
NMD2-TH34	ACGCAGATCTCAGAAGAAGATGATGTTTTTAAC
UPF3-HT1	ACGCGGATCCAAATGAGCAATGTGGCTGGGGAATTG
UPF3-HT2	ACGCGGATCCAAGACAACTTATCAGACTTGGAAAAA
UPF3-HT3	ACGCGGATCCAAAATGAAGAAGACGAAATTTTTAAA
UPF3-HT4	ACGCGGATCCAAAATAAAAACGCCAAAAAGAAATTC
UPF3-HT5	CGCGTCGACCTACTTCTTGGTATCATCACGATG
UPF3-HT6	CGCGTCGACCTATTTCTTCTTTTTGTTCTTATTCTT
UPF3-HT7	CGCGTCGACCTATGTTCCTACTAGCGCGGCATCCTT
UPF3-HT8	CGCGTCGACCTAGAACAAGAAATTGCACCGAGAATA
UPF3-HT9	ACGCGGATCCAAAATGAGACGGTAGATCCTAAAAAG
UPF3-HT10	ACGCGGATCCAAGGTAAATCAACCGAGAATGAAGGA
UPF3-1	TGCTCTAGATACTTGATAGGATTTTATTGCCGT
UPF3-2	CCGCTCGAGATGAGCAATGTGGCTGGGGAATTG
UPF3-3	GATGTTTGAGTGAATTTCTTTACG
UPF3-8	CGAAGATCTGATAGATTACTATATATTTCAGCA
UPF3-9	CGAAGATCTTAAAAGCTCATGGCTTCTTATATA
UPF3-10	CGCGTCGACTCAGTTAAGATAGCATTCATTTGT
UPF3-11	GTAATCCATGGTAGATTACTATATATTTCAGCAGAA
UPF3-12	CGTAAGATGGCAAAAAATTCATCTGCA
UPF3-FLAG	TCTACCATGGATTACAAGGACGACGATGACAAGATGAGCAATGTGGCTGGGAATTG
GAL4(AD)-HIII	CGCAAGCTTTGCAAAGATGGATAA
GAL4(AD)-BamHI	CGCGGATCCCTCTTTTTTTGGGTTTGGTGGGGT
ADH1p-XbaI	GATCTCTAGAGCTTGCATGCAACTTCTTTTCTT
ADH1p-NcoI	GACTCCATGGTTGCAAAGCTTGGAGTTGATTGT

(iv) *lexA*(DB)-*UPF3* and *GAL4*(AD)-*UPF3* fusion constructs. All *lexA*(DB)-*UPF3* fusions used for mapping the Nmd2p- and Upf1p-interacting domains of Upf3p were constructed by using PCR-derived fragments. In each case, a pair of oligonucleotide primers containing either a *Bam*HI site (5′ primer) or a *Sal*I site (3′ primer) were used for amplification (Table 1). The PCR-amplified fragment was digested with *Bam*HI and *Sal*I and ligated into pBTM116 digested previously with *Bam*HI and *Sal*I. The resulting plasmids each carried a distinct fragment from the *UPF3* coding region (Table 4). All *GAL4*(AD)-*UPF3* fusions were constructed in the same way as the *lexA*(DB)-*UPF3* fusions, except that each PCR-derived *Bam*HI-*Sal*I fragment was ligated into pGAD-C2 digested previously with *Bam*HI and *Sal*I. The plasmid pHF1686, isolated from a two-hybrid screen by using *lexA*(DB)-*NMD2*^{DN}(326–1089) as bait, carries a *GAL4*(AD)-*UPF3* fusion including 0.7 kb of *UPF3* C-terminal coding sequences (from codon 152 to the translational stop codon) and 1.3 kb distal to the *UPF3* stop codon.

(v) *GAL4*(AD)-ΔNLS-*NMD2* fusion constructs. *GAL4*(AD)-ΔNLS-*NMD2* fusions each containing an N-terminal deletion of Nmd2p, and the *GAL4*(AD)-ΔNLS-*NMD2* fusions each containing Nmd2p internal fragments beginning at codon 564, were constructed in the same way. In each case, a *Bam*HI-*Sal*I *NMD2* fragment isolated from the corresponding *lexA*(DB)-*NMD2* fusion plasmid was ligated into pACTII-ΔNLS digested previously with *Bam*HI-*Sal*I. The plasmid pACTII-ΔNLS was constructed by a three-fragment ligation, as follows. A 0.4-kb *Hin*dIII-*Bam*HI fragment [containing the *GAL4*(AD)-ΔNLS] PCR amplified from pACTII-*NMD2*^{DN} (14) and a 1.1-kb *Bam*HI-*Sal*I fragment (containing the *ADH1* terminator) isolated from pACTII were ligated into pACTII digested

TABLE 2. Yeast strains

Strain	Genotype	Source (reference)
GGY1::171	*his3 leu2 URA3::GAL1-lacZ gal4*Δ *gal80*Δ	Stanley Fields
L40	*MAT***a** *ade2 his3*Δ*200 leu2-3,112 trp1-901 LYS2::(lexAop)$_4$-HIS3 URA3::(lexAop)$_8$lacZ gal4 gal80*	Stanley Hollenberg
HFY869	Same as L40 but containing *upf1::HIS3*	This study
HFY863	Same as L40 but containing *nmd2::HIS3*	This study
HFY866	Same as L40 but containing *upf3::HIS3*	This study
HFY1200	*MAT***a** *ade2-1 his3-11,15 leu2-3,112 trp1-1 ura3-1 can1-100 UPF1 NMD2 UPF3*	He and Jacobson (12)
HFY870	*MAT***a** *ade2-1 his3-11,15 leu2-3,112 trp1-1 ura3-1 can1-100 upf1::HIS3 NMD2 UPF3*	This study
HFY1300	*MAT*α *ade2-1 his3-11,15 leu2-3,112 trp1-1 ura3-1 can1-100 UPF1 nmd2::HIS3 UPF3*	He and Jacobson (12)
HFY861	*MAT***a** *ade2-1 his3-11,15 leu2-3,112 trp1-1 ura3-1 can1-100 UPF1 NMD2 upf3::HIS3*	This study
HFY3000	*MAT*α *ade2-1 his3-11,15 leu2-3,112 trp1-1 ura3-1 can1-100 upf1::URA3 nmd2::HIS3 UPF3*	He and Jacobson (12)
HFY872	*MAT***a** *ade2-1 his3-11,15 leu2-3,112 trp1-1 ura3-1 can1-100 upf1-1::URA3 NMD2 upf3::HIS3*	This study
HFY874	*MAT***a** *ade2-1 his3-11,15 leu2-3,112 trp1-1 ura3-1 can1-100 UPF1 nmd2::URA3 upf3::HIS3*	This study
HFY883	*MAT***a** *ade2-1 his3-11,15 leu2-3,112 trp1-1 ura3-1 can1-100 upf1::LEU2 nmd2::URA3 upf3::HIS3*	This study

previously with *Hin*dIII and *Sal*I. This led to a replacement of the *GAL4*(AD) by the *GAL4*(AD)-ΔNLS and a change of reading frame at the *Bam*HI site from XGG ATC CGA to GGA TCC GXX. The latter *Bam*HI site is in the same frame as that of pGAD-C1. The oligonucleotide primers *GAL4*(AD)-HIII and *GAL4*(AD)-BamHI were used for PCR amplification (Table 1). All *GAL4*(AD)-ΔNLS-*NMD2* fusions containing C-terminal deletions of Nmd2p were constructed by three-fragment ligations. In each case, a 0.7-kb *Hin*dIII-*Cla*I fragment isolated from the original dominant-negative fragment of *NMD2* [containing the *GAL4*(AD) and a portion of *NMD2*)] and a *Cla*I-*Sal*I fragment isolated from the C-terminal regions of the individual HA-*nmd2* alleles harboring distinct C-terminal deletions (Table 3) were ligated into pACTII previously digested with *Hin*dIII and *Sal*I. Transcription of all of these gene fusions was driven by the potent *ADH1* promoter.

TABLE 3. Plasmids containing *UPF1*, *NMD2*, and *UPF3* alleles

Plasmid	Vector and *UPF1*, *NMD2*, and *UPF3* allele[a]
pHF1390	Bs-*upf1*Δ*CDS* (*Eco*RI-*Bgl*II/*Bgl*II-*Cla*I-*Sal*I)
pHF1395	Bs-*upf1::HIS3*
pHF1397	Bs-*upf1-1::URA3*
pHF275	Bs-*nmd2::URA3*
pHF1201	Bs-*NMD2*(326–391)(E-C)
pHF1203	Bs-*NMD2*^{DN}(326–1089)(E-S)
pHF1628	pRS313-ADH1p-HA-*NMD2*(X-S)
pHF1629	pRS313-ADH1p-HA-*nmd2-C*Δ*166* (deletion of 166 aa from the C terminus)
pHF1630	pRS313-ADH1p-HA-*nmd2-C*Δ*526* (deletion of 526 aa from the C terminus)
pHF1648	pRS313-ADH1p-HA-*nmd2*(564–1089) (encoding residues 564 to 1089)
pHF1520	pRS316-HA-*nmd2-N*Δ*771* (deletion of 771 aa from the N terminus)
pHF1207	pRS316-HA-*nmd2-C*Δ*206* (deletion of 206 aa from the C terminus
pHF1342	pRS316-HA-*nmd2-C*Δ*286* (deletion of 286 aa from the C terminus)
pHF1301	pRS316-HA-*nmd2-C*Δ*318* (deletion of 318 aa from the C terminus)
pHF1338	pRS316-HA-*nmd2-c*Δ*397* (deletion of 397 aa from the C terminus)
pHF1298	pRS316-HA-*nmd2-C*Δ*452* (deletion of 452 aa from the C terminus)
pHF1296	pRS316-HA-*nmd2-C*Δ*526* (deletion of 526 aa from the C terminus)
pHF1569	pRS316-ADH1p-HA-*nmd2*(564–1089) (encoding residues 564 to 1089)
pHF1085	YEplac112-ADH1p-HA-*NMD2*(X-S)
pHF1286	Bs-*upf3*Δ*CDS* (*Xba*I-*Bgl*II/*Bgl*II-*Sal*I)
pHF1409	Bs-*upf3::HIS3*
pHF1288	pRS314-*UPF3*(B-S)
pHF1292	pRS316-*UPF3*(X-S)
pHF1385	pRS316-FLAG-*UPF3*(X-S)
pHF1427	YEplac112-*UPF3*(X-S)
pHF1403	YEplac112-ADH1p-FLAG-*UPF3*(X-S)
pHF1463	YEplac112-ADH1p-HA-*UPF3*(X-S)

[a] aa, amino acids.

(vi) Construction of *upf1::HIS3*, *upf1-1::URA3*, *nmd2::URA3*, and *upf3::HIS3* alleles. The plasmids pHF1395 and pHF1397, which carry the *upf1::HIS3* and *upf1-1::URA3* alleles, respectively, were constructed in two steps. First, a 401-bp PCR-derived *Eco*RI-*Bgl*II fragment containing the promoter and 5′ untranslated region (5′-UTR) of *UPF1* and a 449-bp PCR-derived *Bgl*II-*Sal*I fragment containing sequences 3′ to the translational stop codon of *UPF1* were ligated into Bluescript digested previously with *Eco*RI and *Sal*I. The oligonucleotide pairs *UPF1*-DS1/*UPF1*-DS2 and *UPF1*-DS3/*UPF1*-DS4 were used for PCR amplification of the two fragments, respectively, and this three-fragment ligation reaction generated pHF1390. Second, a 1.8-kb *Bam*HI-*Bam*HI *HIS3* fragment or a 1.2-kb *Bam*HI-*Cla*I *URA3* fragment was ligated into pHF1390 digested previously with *Bgl*II or *Bgl*II and *Cla*I, respectively. This led to a replacement of the entire *UPF1* coding region by either the *HIS3* or *URA3* gene. The plasmid pHF275, which carries the *nmd2::URA3* allele, was also constructed in two steps. First, a 1.1-kb *Xba*I-*Bam*HI fragment containing the promoter, the 5′-UTR, and a portion of the N-terminal coding sequences of *NMD2* was isolated from pRS315-*NMD2*(X-S) (14) and ligated into Bluescript digested previously with *Xba*I and *Bam*HI, generating Bs-*NMD2*(X-B). Second, a 1.2-kb *Bam*HI-*Cla*I *URA3* fragment and a 1.1-kb *Cla*I-*Eco*RI fragment from the *NMD2* coding region were ligated into Bs-*NMD2*(X-B) digested previously with *Bam*HI and *Eco*RI. This led to a replacement of the *NMD2* coding region from the *Bam*HI site to the *Cla*I site by the *URA3* gene. Plasmid pHF1409, carrying the *upf3::HIS3* allele, was constructed in the same way as pHF1395 except that a 433-bp PCR-derived *Xba*I-*Bgl*II fragment (containing the promoter and 5′-UTR of *UPF3*) and a 381-bp PCR-derived *Bgl*II-*Sal*I fragment (containing sequences 3′ to the translational stop codon of *UPF3*) were ligated into Bluescript digested previously with *Xba*I and *Sal*I in a three-fragment ligation reaction, generating pHF1286. The oligonucleotide pairs *UPF3*-1/*UPF3*-8 and *UPF3*-9/*UPF3*-10 were used for PCR amplification of the respective fragments.

(vii) *NMD2*-containing plasmids. The plasmids pHF1207 and pHF1206, which carry HA-*nmd2* alleles encoding C-terminal Nmd2p deletions of 206 and 273 residues, respectively, were constructed by using pHF926 (14). In either case, a PCR-derived *Eco*RI-*Bgl*II fragment was ligated into pHF926 digested previously with *Eco*RI and *Bgl*II. This led to a replacement of the wild-type *NMD2* fragment (from the *Eco*RI site in the coding region to the translation stop codon) by a C-terminally truncated one. The oligonucleotide pairs *NMD2*-M11/*NMD2*-TH23 and *NMD2*-M11/*NMD2*-TH22 were used for PCR amplification of the respective fragments. The plasmids pHF1342, pHF1301, pHF1338, pHF1298, and pHF1296, which carry HA-*nmd2* alleles containing C-terminal deletions of 286, 318, 397, 452, and 526 codons, respectively, were constructed in the same way as pHF1207 and pHF1206. In each case, a PCR-derived *Cla*I-*Bgl*II fragment was ligated into pHF926 digested previously with *Cla*I and *Bgl*II. This led to a replacement of the wild-type *NMD2* fragment (from the *Cla*I site in the coding region to the translation stop codon) by a C-terminally truncated one. The oligonucleotide pairs hf21′-1/*NMD2*-TH5, hf21′-1/*NMD2*-TH31, hf21′-1/*NMD2*-TH32, hf21′-1/*NMD2*-TH33, and hf21′-1/*NMD2*-TH34 were used for amplification (Table 1) (14). The plasmid pHF1569, which carries the HA-*nmd2*(564–1089) allele, was constructed in two steps. First, the *Xba*I-*Sal*I fragment containing the HA-*nmd2*-NΔ771 allele was isolated from pHF692 (14) and ligated into pRS316, generating pHF1520. Second, an *Eco*RI-*Eco*RI fragment containing *NMD2* sequences from codon 564 to the *Eco*RI site in the coding region was isolated from pHF1309 and ligated into pHF1520 digested previously by *Eco*RI. The plasmid pHF1085, which carries an *ADH1* promoter-driven HA-*NMD2* allele, was constructed by ligating a 431-bp PCR-amplified *Xba*I-*Nco*I fragment, containing the promoter and 5′-UTR of the *ADH1* gene, into YEplac112-HA-*NMD2*(X-S) (12) digested previously with *Xba*I and *Nco*I. This led

TABLE 4. *lexA*(DB), *GAL4*(DB), and *GAL4*(AD) fusion constructs

Plasmid	Vector and relevant sequence	Plasmid	Vector and relevant sequence
pHF1668	pGAD-C1-*UPF1*(1–971)	pHF1672	pGAD-C1-*NMD2*(564–883)
pHF1163	pACTII*-*UPF1*(1–666)	pHF1674	pGAD-C1-*NMD2*(564–816)
pHF1161	pACTII*-*UPF1*(1–555)	pHF1676	pGAD-C1-*NMD2*(564–803)
pHF1159	pACTII*-*UPF1*(1–420)	pHF1534	pGAD-C1-*NMD2*(565–771)
pHF1011	pACTII*-*UPF1*(1–289)	pHF1536	pGAD-C1-*NMD2*(564–692)
pHF1017	pACTII*-*UPF1*(1–207)	pHF1355	pACTII-C1-ΔNLS-*NMD2*(473–1089)
pHF1177	pACTII*-*UPF1*(1–181)	pHF1357	pACTII-C1-ΔNLS-*NMD2*(564–1089)
pHF1175	pACTII*-*UPF1*(1–153)	pHF1359	pACTII-C1-ΔNLS-*NMD2*(638–1089)
pHF1013	pACTII*-*UPF1*(62–289)	pHF1361	pACTII-C1-ΔNLS-*NMD2*(693–1089)
pHF1019	pACTII*-*UPF1*(62–207)	pHF1363	pACTII-C1-ΔNLS-*NMD2*(772–1089)
pHF1181	pACTII*-*UPF1*(62–181)	pHF1365	pACTII-C1-ΔNLS-*NMD2*(817–1089)
PHF1015	pACTII*-*UPF1*(80–289)	pHF1367	pACTII-C1-ΔNLS-*NMD2*(879–1089)
pHF1165	pACTII*-*UPF1*(290–971)	pHF1258	pACTII-ΔNLS-*NMD2*(326–883)
pHF1169	pACTII*-*UPF1*(556–971)	pHF1256	pACTII-ΔNLS-*NMD2*(326–816)
pHF1050	pMA424-*NMD2*(933–1089)	pHF1377	pACTII-ΔNLS-*NMD2*(326–803)
pHF1186	pBTM116-*NMD2*^{DN}(326–1089)	pHF1375	pACTII-ΔNLS-*NMD2*(326–771)
pHF1308	pBTM116-*NMD2*(473–1089)	pHF1373	pACTII-ΔNLS-*NMD2*(326–692)
pHF1309	pBTM116-*NMD2*(564–1089)	pHF1371	pACTII-ΔNLS-*NMD2*(326–637)
pHF1311	pBTM115-*NMD2*(638–1089)	pHF1369	pACTII-ΔNLS-*NMD2*(326–563)
pHF1313	pBTM116-*NMD2*(693–1089)	pHF1493	pACTII-C1-ΔNLS-*NMD2*(564–923)
pHF1268	pBTM116-*NMD2*(772–1089)	pHF1495	pACTII-C1-ΔNLS-*NMD2*(564–883)
pHF1304	pBTM116-*NMD2*(817–1089)	pHF1497	pACTII-C1-ΔNLS-*NMD2*(564–816)
pHF1306	pBTM116-*NMD2*(879–1089)	pHF1499	pACTII-C1-ΔNLS-*NMD2*(564–803)
pHF1270	pBTM116-*NMD2*(933–1089)	pHF1540	pACTII-C1-ΔNLS-*NMD2*(564–771)
pHF1262	pBTM116-*NMD2*(326–923)	pHF1542	pACTII-C1-ΔNLS-*NMD2*(564–692)
pHF1264	pBTM116-*NMD2*(326–883)	pHF1412	pBTM116-*UPF3*(1–387)
pHF1266	pBTM116-*NMD2*(326–816)	pHF1650	pBTM116-*UPF3*(32–387)
pHF1352	pBTM116-*NMD2*(326–803)	pHF1656	pBTM116-*UPF3*(78–387)
pHF1349	pBTM116-*NMD2*(326–771)	pHF1318	pBTM116-*UPF3*(152–387)
pHF1348	pBTM116-*NMD2*(326–692)	pHF1320	pBTM116-*UPF3*(205-–387)
pHF1345	pBTM116-*NMD2*(326–637)	pHF1322	pBTM116-*UPF3*(279–387)
pHF1344	pBTM116-*NMD2*(326–563)	pHF1332	pBTM116-*UPF3*(1–278)
pHF1467	pBTM116-*NMD2*(564–923)	pHF1330	pBTM116-*UPF3*(1–204)
pHF1469	pBTM116-*NMD2*(564–883)	pHF1316	pBTM116-*UPF3*(1–151)
pHF1471	pBTM116-*NMD2*(564–816)	pHF1652	pMTB116-*UPF3*(32–278)
pHF1473	pBTM116-*NMD2*(564–803)	pHF1658	pBTM116-*UPF3*(78–278)
pHF1528	pBTM116-*NMD2*(564–771)	pHF1324	pBTM116-*UPF3*(152–278)
pHF1530	pBTM116-*NMD2*(564–692)	pHF1654	pBTM116-*UPF3*(32–204)
pHF1441	pGAD-C1-*NMD2*^{DN}(326–1089)	pHF1660	pBTM116-*UPF3*(78–204)
pHF1415	pGAD-C1-*NMD2*(473–1089)	pHF1326	pBTM116-*UPF3*(152–204)
pHF1417	pGAD-C1-*NMD2*(564–1089)	pHF1414	pGAD-C2-*UPF3*(1–387)
pHF1419	pGAD-C1-*NMD2*(638–1089)	pHF1636	pGAD-C2-*UPF3*(32–387)
pHF1421	pGAD-C1-*NMD2*(693–1089)	pHF1642	pGAD-C2-*UPF3*(78–387)
pHF1423	pGAD-C1-*NMD2*(772–1089)	pHF1274	pGAD-C2-*UPF3*(152–387)
pHF1425	pGAD-C1-*NMD2*(817–1089)	pHF1276	pGAD-C2-*UPF3*(205–387)
pHF1427	pGAD-C1-*NMD2*(879–1089)	pHF1278	pGAD-C2-*UPF3*(279–387)
pHF1429	pGAD-C1-*NMD2*(933–1089)	pHF1336	pGAD-C2-*UPF3*(1–278)
pHF1458	pGAD-C1-*NMD2*(326–923)	pHF1334	pGAD-C2-*UPF3*(1–204)
pHF1456	pGAD-C1-*NMD2*(326–883)	pHF1272	pGAD-C2-*UPF3*(1–151)
pHF1454	pGAD-C1-*NMD2*(326–816)	pHF1638	pGAD-C2-*UPF3*(32–278)
pHF1452	pGAD-C1-*NMD2*(326–803)	pHF1644	pGAD-C2-*UPF3*(78–278)
pHF1450	pGAD-C1-*NMD2*(326–771)	pHF1280	pGAD-C2-*UPF3*(152–278)
pHF1448	pGAD-C1-*NMD2*(326–692)	pHF1640	pGAD-C2-*UPF3*(32–204)
pHF1446	pGAD-C1-*NMD2*(326–637)	pHF1646	pGAD-C2-*UPF3*(78–204)
pHF1431	pGAD-C1-*NMD2*(326–563)	pHF1282	pGAD-C2-*UPF3*(152–204)
pHF1670	pGAD-C1-*NMD2*(564–923)	pHF1686	pGAD-C1-*UPF3*(152–387)

to a replacement of the *NMD2* promoter region by that of *ADH1*. The oligonucleotides ADH1p-XbaI and ADH1p-NcoI (Table 1) were used for PCR amplification. The plasmids pHF1628, pHF1629, pHF1630, and pHF1648, which carry the *ADH1* promoter-driven HA-*NMD2*, HA-*nmd2-CΔ166*, HA-*nmd2-CΔ526*, and HA-*nmd2*(564–1089) alleles, respectively, were constructed by three-fragment ligations. In each case, a 431-bp *Xba*I-*Nco*I fragment (containing the *ADH1* promoter region) isolated from pHF1085 and an *Nco*I-*Sal*I fragment (containing the respective *NMD2* alleles) isolated from pHF1085, pHF707 (14), pHF1296, and pHF1569, were ligated into pRS313 digested previously with *Xba*I and *Sal*I.

(viii) *UPF3*-containing plasmids. Plasmid pHF1427, which carries a wild-type *UPF3* gene, was constructed by a three-fragment ligation. A PCR-derived *Xba*I-*Sna*BI fragment (containing 427 bp of the promoter region and 559 bp of the N-terminal portion of the *UPF3* coding region) and a 2.0-kb *Sna*BI-*Sal*I fragment (containing sequences including the C-terminal portion of the *UPF3* coding region and the 3′-UTR region), isolated from pHF1686, were ligated into YEplac112 digested previously with *Xba*I and *Sal*I. The oligonucleotide primers *UPF3*-1 and *UPF3*-3 were used in PCR amplification. Plasmids pHF1288 and pHF1292 both carry the wild-type *UPF3* gene and were constructed by ligating either a *Bam*HI-*Sal*I or an *Xba*I-*Sal*I fragment isolated from pHF1427 into pRS314 or pRS316 digested previously with either *Bam*HI and *Sal*I or *Xba*I and *Sal*I, respectively. The plasmid pHF1385, which carries a FLAG-*UPF3* allele, was constructed by using pHF1292. A PCR-derived *Xba*I-*Nco*I fragment (containing the *UPF3* promoter region) and a PCR-derived *Nco*I-*Hin*dIII fragment (containing the FLAG epitope and an N-terminal portion of the *UPF3* coding region)

were ligated into pHF1292 digested previously with *Xba*I and *Hin*dIII. The oligonucleotide pairs *UPF3*-1/*UPF3*-11 and *UPF3*-FLAG/*UPF3*-12 were used for amplification of the respective fragments. The plasmid pHF1403, which carries an *ADH1* promoter-driven FLAG-*UPF3* allele, was constructed by ligating an *Nco*I-*Sal*I fragment (containing the FLAG-*UPF3* allele), isolated from pHF1385, into pHF1085 digested previously with *Nco*I and *Sal*I. Plasmid pHF1463, which carries an *ADH1* promoter-driven HA-*UPF3* allele, was constructed by ligating a PCR-derived *Xho*I-*Sal*I fragment (containing the entire *UPF3* coding region and approximately 0.4 kb from its 3′-UTR) into pHF1085 digested previously with *Xho*I and *Sal*I. The oligonucleotide primers *UPF3*-2 and *UPF3*-10 were used for PCR amplification.

Two-hybrid screening. The yeast strain L40 was cotransformed with both pHF1186 [carrying the *lexA*(DB)-*NMD2*^{DN}(326–1089) fusion] and one of the libraries containing genomic DNA fragments fused to the *GAL4*(AD). Transformants were grown for 10 h in synthetic liquid medium lacking tryptophan and leucine to maintain selection for the *lexA-NMD2*^{DN}(326–1089) fusion plasmid and the library plasmid, respectively. The transformants were then plated on synthetic medium lacking histidine, tryptophan, and leucine and containing 5 mM 3-aminotriazole. After 4 to 6 days of growth on plates at 30°C, His$^+$ transformants were replica plated to X-Gal (5-bromo-4-chloro-3-indolyl-β-D-galactopyranoside) plates and were incubated until blue colonies appeared. Library plasmids were recovered from blue colonies as previously described (12). To test for specificity, isolated library plasmids were individually retransformed into the original L40 strain with either (i) the *lexA*(DB)-*NMD2*^{DN} fusion, (ii) a series of the *lexA*(DB)-*NMD2*^{DN} fusions containing deletions from the C terminus, or (iii) the *lexA*(DB) vector only. The plasmids encoding Nmd2^{DN}p-interacting proteins were characterized further by sequence analysis. DNA sequences were compared to existing sequence databases by using the BlastN program (2).

Two-hybrid interaction assay. The two-hybrid tester strain GGY1::171 was used to assay interactions between Upf1p and Nmd2p. The two-hybrid tester strain L40 was used to assay interactions between Nmd2p and Upf3p and between Upf1p and Upf3p. In each case, a *GAL4*(DB) or *lexA*(DB) fusion construct (Table 4) was cotransformed with a *GAL4*(AD) construct into the tester strain. Transformants were incubated for 3 to 5 days at 30°C until colonies were fairly large. Both qualitative and quantitative assays for β-galactosidase activity were performed as previously described (14, 24). Cells harboring each of the pGAD-C1, pGAD-C2, pACTII, pMA424, and pBTM116 vectors produced <0.05 U of β-galactosidase activity. Values for β-galactosidase assays represent the means for at least three independent transformants. Standard deviations are indicated.

RNA preparation and Northern analysis. RNA preparation and Northern analysis were performed as previously described (14). The ratio of *CYH2* pre-mRNA to mRNA was used as an index of the activity of the nonsense-mediated mRNA decay pathway (12–14). The values presented represent averages from at least two independent experiments.

Western blot analysis. Western blot analyses, performed as previously described (14), were used to monitor fusion protein expression levels. An antihemagglutinin (anti-HA) monoclonal antibody (12CA5; Boehringer) was diluted 1:1,000. Horseradish peroxidase-conjugated goat anti-mouse immunoglobulin G-immunoglobulin M (heavy plus light chains) was diluted 1:5,000. Bound antibodies were detected with the enhanced chemiluminescence system (Amersham) used according to the manufacturer's instructions.

RESULTS

Identification of Upf1p and Upf3p as proteins that interact with a dominant-negative fragment of Nmd2p. We previously demonstrated that overexpression of a *GAL4*(AD) fusion to a 764-amino-acid C-terminal fragment of Nmd2p (Nmd2^{DN}p) inhibits the nonsense-mediated mRNA decay pathway in a dominant manner when the fusion protein is localized to the cytoplasm but not when it is localized to the nucleus (12). Amino acid substitutions or deletions in the Upf1p-interacting domain of this protein do not affect dominant-negative inhibition of mRNA decay, suggesting that Nmd2^{DN}p interacts not only with Upf1p but also with at least one additional factor (14). To identify potential Nmd2^{DN}p-interacting factors, we used the yeast two-hybrid system (10, 39). DNA encoding the dominant-negative *NMD2*^{DN} allele was inserted into a yeast expression vector in frame with a sequence encoding the DNA-binding domain of the *lexA* protein. This plasmid was introduced into the yeast strain L40 (15), which harbors the *HIS3* and *lacZ* genes under the control of promoters containing the *lexA*-binding site. Yeast genomic DNA libraries fused, in three separate frames, to sequences encoding the Gal4p transcriptional activation domain were then screened for cotransforming plasmids which allow the L40 cells to express these two reporter genes.

Approximately 3×10^6 independent transformants were screened, and 90 colonies that grew in the absence of histidine and in the presence of 5 mM 3-aminotriazole and exhibited β-galactosidase activity were isolated. The library plasmids from these colonies were rescued and tested for specificity by retransforming them into the original L40 strain simultaneously with either (i) the *lexA*(DB)-*NMD2*^{DN} fusion, (ii) a series of the *lexA*(DB)-*NMD2*^{DN} fusions containing deletions from the C terminus, or (iii) the *lexA*(DB) vector only. Restriction mapping and partial DNA sequence analysis of plasmids which passed these specificity tests yielded seven different genes encoding putative Nmd2^{DN}p-interacting proteins. One class of clones, as we expected, encoded near-full-length Upf1p, and a second class of clones encoded a fragment of 236 amino acids from the C terminus of Upf3p (19). The other five classes of clones encoded either previously identified genes (*SPP41* and *RED1*) (23, 36) or uncharacterized open reading frames (YBR270c, YKL023w, and YNR023w). Deletion of *RED1* does not affect nonsense-mediated mRNA decay (data not shown), and the roles of the other four genes have yet to be determined. In the experiments described below, we have characterized the interactions between the three principal components of the nonsense-mediated mRNA decay pathway, i.e., Upf1p, Nmd2p, and Upf3p.

Upf1p and Upf3p interact with distinct domains of Nmd2p. To determine the regions of Nmd2p responsible for interaction with Upf1p and Upf3p, we constructed a series of *NMD2* deletions and tested their abilities to promote two-hybrid interactions with either *UPF1* or *UPF3*. *NMD2* fragments were fused in frame to the *lexA*(DB), and the full-length *UPF1* and *UPF3* genes were fused in frame to the *GAL4*(AD). The extent of interaction between the respective fusion proteins was monitored in cotransformants indirectly, by both a qualitative plate assay and a quantitative solution assay for β-galactosidase. These experiments established that coexpression of *GAL4*(AD)-*UPF1* with all of the *lexA*(DB)-*NMD2* fusions that included the 157 C-terminal amino acids of Nmd2p led to the accumulation of substantial β-galactosidase activity (Fig. 1, constructs 1 to 9), whereas coexpression of *GAL4*(AD)-*UPF1* with all of the *lexA*(DB)-*NMD2* fusions that lack 166 or more C-terminal amino acids from Nmd2p yielded background levels of β-galactosidase activity (Fig. 1, constructs 10 to 23). These results, and earlier studies using different DNA-binding domain and activation domain fusion constructs (14), support our previous conclusion that Upf1p interacts with a 157-amino-acid C-terminal domain of Nmd2p (14) and demonstrate that Upf1p-Nmd2p two-hybrid interactions are independent of the nature of the DNA-binding domain and activation domain fusions utilized. The decreased levels of β-galactosidase activity obtained with three fusions that retain an intact Nmd2p C terminus (Fig. 1, constructs 2, 4, and 5) are not indicative of additional Upf1p-interacting epitopes but rather reflect the instability of the respective fusion proteins (data not shown).

Cells coexpressing the full-length *GAL4*(AD)-*UPF3* fusion and the *lexA*(DB)-*NMD2*^{DN}(326–1089) fusion accumulated substantially less β-galactosidase activity than the corresponding Nmd2p-Upf1p fusion pair but nevertheless accumulated sufficient activity to indicate interaction (Fig. 1, construct 1). This activity doubled when amino acids 326 to 563 were deleted from Nmd2p (Fig. 1, construct 3) and was eliminated when the DNA-binding domain fusion included only amino acids 326 to 563 of Nmd2p (Fig. 1, construct 17). These data suggest that the region of Nmd2p from residue 564 to 1089 must contain the entire Upf3p-interacting domain. To map this

A

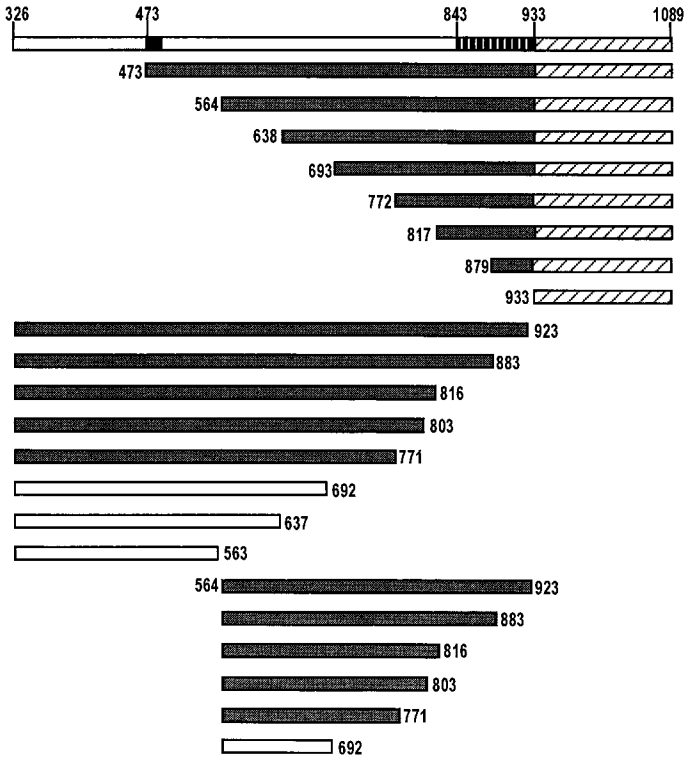

	Upf1p Interaction	Upf3p Interaction	Dominant Inhibition
1	120.0 ± 8.7	5.6 ± 0.7	0.54
2*	7.5 ± 0.7	0.2 ± 0.0	0.30
3	142.8 ± 13.5	10.4 ± 1.3	0.48
4*	43.7 ± 3.7	0.1 ± 0.1	0.13
5*	53.3 ± 3.3	0.1 ± 0.1	0.14
6	136.5 ± 6.9	0.3 ± 0.1	0.12
7	116.0 ± 3.8	0.3 ± 0.1	0.12
8	128.3 ± 5.8	0.3 ± 0.1	0.10
9	124.5 ± 7.4	≤ 0.05	0.10
10	≤ 0.05	5.4 ± 0.3	0.48
11	≤ 0.05	1.2 ± 0.2	0.51
12	≤ 0.05	1.2 ± 0.1	0.48
13	≤ 0.05	1.0 ± 0.2	0.20
14	≤ 0.05	1.0 ± 0.3	0.14
15	≤ 0.05	≤ 0.05	0.13
16*	≤ 0.05	≤ 0.05	0.10
17	≤ 0.05	≤ 0.05	0.14
18	≤ 0.05	8.2 ± 0.6	0.47
19	≤ 0.05	3.0 ± 0.4	0.48
20	≤ 0.05	2.7 ± 0.4	0.47
21	≤ 0.05	2.2 ± 0.4	0.15
22	≤ 0.05	2.0 ± 0.3	0.13
23	≤ 0.05	≤ 0.05	0.12

domain further, the consequences of both N-terminal and C-terminal deletions of Nmd2p were analyzed. The results obtained from this experiment indicate the following (i) Upf3p interacts with an Nmd2p domain that is distinct from the Upf1p-interacting domain, since a construct containing only the latter did not interact with Upf3p (Fig. 1, construct 9) and deletion of the Upf1p-interacting domain of Nmd2p had no effect on its interaction with Upf3p (Fig. 1, constructs 10 and 18; compare to constructs 1 and 3). (ii) The region encompassed by Nmd2p residues 564 to 771 contains a major determinant for Upf3p interaction, since the *lexA*(DB)-*NMD2*(772–1089) fusion containing an N-terminal deletion from residue 564 to 771 led to a large decrease of β-galactosidase activity (Fig. 1, construct 6), the *lexA*(DB)-*NMD2* fusions containing this region yielded substantial levels of β-galactosidase activity (Fig. 1, constructs 10 to 14 and 18 to 22), and fusion proteins with C-terminal truncations of this region lost all detectable Upf3p interaction activity (Fig. 1, constructs 15 and 23). The actual N-terminal boundary of this interacting domain could not be determined because two of the *NMD2* fusion proteins (Fig. 1, constructs 4 and 5) were unstable, regardless of whether the fusions were to the *lexA*(DB) or the *GAL4*(AD) (data not shown). (iii) The region of Nmd2p from residue 879 to 933 that contains almost the entire acidic domain of Nmd2p (12, 14) contributes to Upf3p interaction, since deletion of this region from the respective fusion proteins leads to reduced levels of β-galactosidase activity (Fig. 1, compare construct 10 to 11 and construct 18 to 19) and since the *lexA*(DB)-*NMD2*(879–1089) fusion yielded detectable levels of β-galactosidase activity (Fig. 1, construct 8). (iv) The region of Nmd2p from residue 772 to 878 may not contribute to interaction with Upf3p, since N- or C-terminal deletions into this region had almost no effect on Nmd2p-Upf3p two-hybrid interaction (Fig. 1, constructs 6 to 8, 11 to 14, and 19 to 22).

Interactions between Upf3p and Nmd2p were also examined in constructs in which the respective activation domain and DNA-binding domain fusions were reversed. In support of the conclusions delineated above, results qualitatively identical to those presented in Fig. 1 were obtained (data not shown).

An internal domain of Upf3p encompassing residues 78 to 278 is the major determinant for interaction with Nmd2p. *UPF3* was identified as a gene encoding an $Nmd2^{DN}$p-interacting protein (see above), and the respective Upf3p region(s) responsible for such interaction was determined by analyzing the activities of deletion derivatives in the two-hybrid system. *UPF3* fragments were fused in frame to the *lexA*(DB), and the *NMD2* fragment that contains the entire Upf3p-binding site, i.e., that from residue 564 to 1089 (Fig. 1), was fused in frame to the *GAL4*(AD). As shown in Fig. 2, coexpression of the *GAL4*(AD)-*NMD2*(564–1089) fusion with either the full-length *lexA*(DB)-*UPF3* fusion (Fig. 2, construct 1) or *lexA*(DB)-*UPF3* fusions containing N-terminal deletions of either 31 or 77 amino acids (Fig. 2, constructs 2 and 3) yielded substantial levels of β-galactosidase activity. A *lexA*(DB) fusion containing a deletion of 151 amino acids from the Upf3p N terminus led to a significant decrease of β-galactosidase activity (Fig. 2, construct 4), and fusions containing deletions of either 204 or 279 amino acids from the Upf3p N terminus

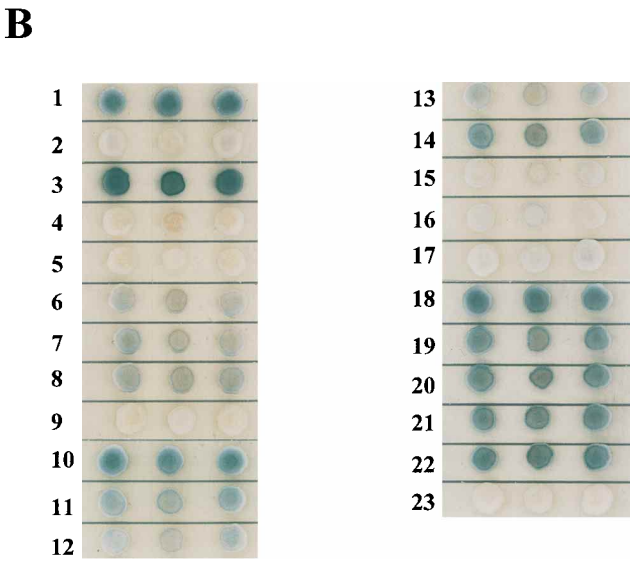

FIG. 1. Two-hybrid interactions and dominant-negative activities of Nmd2p fragments. (A and B). Upf1p, Upf3p, and at least one other factor interact with distinct regions of Nmd2p. The yeast two-hybrid system was used to identify the Upf1p- and Upf3p-interacting domains within Nmd2p, using the tester strain L40. A *GAL4*(AD)-*UPF1*(1–971) fusion and a *GAL4*(AD)-*UPF3*(1–387) fusion were used to test for interactions with each of 23 *lexA*(DB)-*NMD2* fusions encoding distinct fragments of Nmd2p. Individual transformants were selected, and β-galactosidase activity was determined (see Materials and Methods). (A) Quantitative liquid assay for β-galactosidase activity. *NMD2* sequences fused to the *lexA*(DB) are illustrated on the left. The small black box represents the putative transmembrane helix (14), and the hatched black and hatched open boxes represent the acidic and the Upf1p-interacting domains, respectively. The grey and open boxes in constructs 2 to 23 represent *lexA*(DB)-*NMD2* fusions that, respectively, do or do not interact with Upf3p. Upf1p Interaction and Upf3p Interaction depict the respective β-galactosidase activities (means ± standard deviations) for at least three independent assays performed on cultures derived from individual colonies. Dominant Inhibition depicts the ratio of *CYH2* pre-mRNA to mRNA determined in panel C by Northern blotting. Asterisks depict fusion proteins shown by Western blotting to be significantly less abundant than that encoded by construct 1. (B) Qualitative β-galactosidase assay, on X-Gal-containing plates, for Upf3p interaction only. (C) Identification of regions of Nmd2p responsible for dominant-negative inhibition. Each of the *NMD2* fragments shown in panel A was fused in frame to a *GAL4*(AD) in which the nuclear localization signal had been deleted. Total RNA was isolated from HFY1200 (a wild-type *NMD2* strain) overexpressing each of the respective fusion proteins. RNA was fractionated by gel electrophoresis and analyzed by Northern blotting, using the 0.6-kb *Eco*RI-*Hin*dIII fragment of the *CYH2* gene as a probe. Lanes: WT, RNA from HFY1200 harboring pACTII(ΔNLS) only; 1 to 23, RNAs from HFY1200 overexpressing each of the *GAL4*(AD)-*NMD2* fusion proteins that contain the corresponding fragments shown in panel A. *CYH2* pre-mRNA/mRNA ratios from the blot are summarized in the last column of panel A.

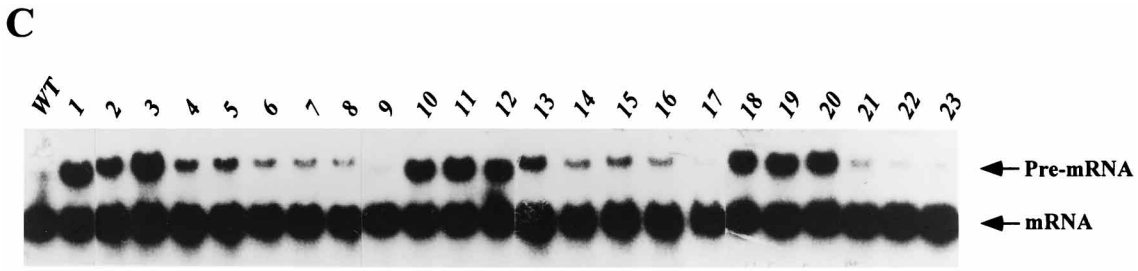

yielded background levels of β-galactosidase activity (Fig. 2, constructs 5 and 6). Comparable effects of N-terminal deletions were observed with Upf3p fragments that also contain C-terminal truncations (Fig. 2, constructs 7, 10, and 11 and constructs 8, 13, and 14). These results indicate that (i) two regions of Upf3p, from residue 78 to 151 and from residue 152 to 204, must contain important Nmd2p-interacting epitopes and (ii) the N-terminal 77 amino acids of Upf3p do not contribute to the interaction with Nmd2p, and their presence in the fusion proteins may inhibit such an interaction to some extent.

C-terminal deletions of *UPF3* provided further definition of its Nmd2p-interacting domain. *lexA*(DB)-*UPF3* fusions containing C-terminal deletions of 109 or 183 amino acids promoted almost twofold increases in β-galactosidase activity, relative to that of the full-length fusion (Fig. 2, constructs 7 and 8), whereas the fusion containing a deletion of 236 amino acids from the Upf3p C terminus yielded background levels of β-galactosidase (Fig. 2, construct 9). These results underscore the importance of Upf3p residues 152 to 204 in Nmd2p binding. Moreover, these results, and those demonstrating the consequences of C-terminal truncation of Upf3p fragments which also contain N-terminal deletions (Fig. 2, constructs 10 to 15), further suggest that the C-terminal 109 amino acids of Upf3p do not contribute to Nmd2p interaction and may actually inhibit Nmd2p-Upf3p interaction. Taken together, the results in Fig. 2 indicate that the region of Upf3p from residue 78 to 204 is necessary for Nmd2p interaction.

Interactions between Upf3p and Nmd2p were also examined in constructs in which the *lexA*(DB) and *GAL4*(AD) fusions were reversed. Results essentially identical to those shown in Fig. 2 were obtained except that we did detect a weak interaction between *lexA*(DB)-*NMD2*(564–1089) and a *GAL4*(AD)-*UPF3* fusion containing a deletion of 204 amino acids from its N terminus (the latter being the homolog of construct 5 in Fig. 2) (data not shown). This observation suggests that the region from Upf3p residue 205 to 279 may also contribute to Upf3-Nmd2p interaction, a conclusion further supported by the observation that the *lexA*(DB) fusion harboring *UPF3* residues 78 to 278 demonstrated the highest level of β-galactosidase activity when tested for interaction with *GAL4*(AD)-*NMD2*(564–1089) (Fig. 2, construct 11). Thus, we conclude that an internal region of Upf3p, comprised of residues 78 to 278, is the major determinant for interaction with Nmd2p.

The Zn^{2+} finger-like motifs in Upf1p are necessary but not sufficient for interaction with Nmd2p. We previously identified *NMD2* as a gene encoding a Upf1p-interacting protein and localized its Upf1p-interacting domain to a 157-amino-acid segment at its carboxyl terminus (12, 14). To determine the region(s) of Upf1p responsible for interaction with Nmd2p, we constructed a series of Upf1p deletion derivatives and tested their abilities to interact with Nmd2p in the two-hybrid system.

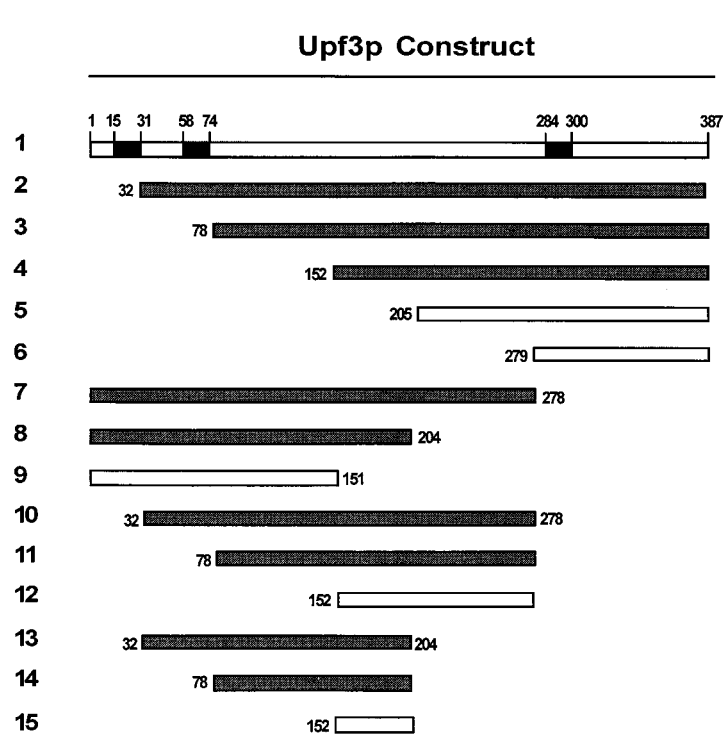

	Nmd2p Interaction	Upf1p Interaction	
		a	b
1	25.6±5.2	0.4±0.0	99.5±17.0
2	27.7±3.6	9.2±0.7	92.3±9.1
3	42.0±1.1	6.6±0.5	120.3±25.0
4	7.4±0.7	0.1±0.0	58.1±1.3
5	≤0.05*	≤0.05	≤0.05
6	≤0.05	≤0.05	≤0.05
7	49.2±1.6	23.3±4.5	153.4±17.8
8	54.7±5.0	≤0.05	161.6±4.4
9	≤0.05	≤0.05	≤0.05
10	48.9±3.5	25.9±4.3	90.7±12.2
11	89.4±3.2	27.7±2.5	85.4±9.5
12	≤0.05	≤0.05	≤0.05
13	49.8±5.6	0.9±0.1	165.6±16.5
14	34.9±1.1	≤0.05	40.9±5.8
15	≤0.05	≤0.05	≤0.05

FIG. 2. Identification of Upf1p- and Nmd2p-interacting domains within Upf3p. The yeast two-hybrid system was used to identify the Upf1p- and Nmd2p-interacting domains within Upf3p, using the tester strain L40. A *GAL4*(AD)-*NMD2*(564–1089) fusion and a *GAL4*(AD)-*UPF1*(1–971) fusion were used to test for interaction with each of 15 *lexA*(DB)-*UPF3* fusions encoding distinct fragments of Upf3p (Nmd2p Interaction and Upf1p Interaction [column a], respectively). Interaction between the *GAL4*(AD)-*UPF1*(1–971) fusion and each of the *lexA*(DB)-*UPF3* fusions was also assayed with strain L40 harboring a plasmid that overexpresses a fragment of *NMD2* from residue 564 to 1089 (Upf1p Interaction [column b]). Individual transformants were selected, and β-galactosidase activity was determined quantitatively in a liquid assay. *UPF3* sequences fused to the *lexA*(DB) are illustrated. The black boxes in construct 1 represent the three putative bipartite nuclear localization signals. The grey and open boxes in constructs 2 to 15 represent *lexA*(DB)-*UPF3* fusions that, respectively, do or do not interact with Nmd2p. Interaction values depict mean β-galactosidase activities ± standard deviations for at least three independent assays performed on cultures derived from individual colonies. The asterisk in the Nmd2p interaction column for construct 5 indicates that weak β-galactosidase activity was detected from this construct when the AD and DB vectors were reversed.

Here, the *UPF1*-containing fragments were fused in frame to the *GAL4*(AD), and the *NMD2* fragment that contains the entire Upf1p-interacting domain (residues 933 to 1089) was fused in frame to the *GAL4*(DB). As shown in Fig. 3, coexpression of the *GAL4*(DB)-*NMD2*(933–1089) fusion with full-length *GAL4*(AD)-*UPF1* (Fig. 1, construct 1) or *GAL4*(AD) fusions harboring *UPF1* fragments with C-terminal deletions up to residue 181 (Fig. 3, constructs 2 to 7) all led to the accumulation of substantial β-galactosidase activity. *GAL4* (AD) fusions harboring internal *UPF1* fragments from residues 62 to 289, 62 to 207, and 62 to 181 (Fig. 3, constructs 9 to 11) also showed significant two-hybrid activity, but that activity was three- to sixfold less than that of the aforementioned *UPF1* fusions. This decrease in activity was specific for interaction with Nmd2p, since the same deletions had no effect on Upf1p homodimerization (12a). In contrast, no detectable β-galactosidase activity was observed when the *GAL4*(DB)-*NMD2*(933–1089) fusion was coexpressed with (i) a *GAL4*(AD) fusion harboring a *UPF1* fragment with a C-terminal deletion up to residue 153 (Fig. 3, construct 8), (ii) *GAL4*(AD) fusions harboring *UPF1* fragments with N-terminal deletions of either 290 or 556 residues (Fig. 3, constructs 13 and 14), or (iii) *GAL4*(AD) fusions harboring internal *UPF1* fragments from residues 62 to 153 (data not shown), 80 to 289 (Fig. 3, construct 12), 80 to 207, and 80 to 181 (data not shown). These results indicate that the N-terminal 181 amino acids of Upf1p contain the major determinant(s) for interaction with Nmd2p. This region includes, but is not limited to, amino acids comprising the Zn^{2+} finger-like motifs within Upf1p (1, 18, 22), indicating that they are essential but not sufficient for interaction with Nmd2p. These conclusions were substantiated by observations that internal deletions of Upf1p from residue 62 to 152 or 152 to 289 completely abolished Upf1p-Nmd2p interaction while deletions of residues 290 to 425, 426 to 553, 554 to 608, 609 to 789, and 790 to 806 had essentially no effect on such interaction (data not shown).

Upf1p and Upf3p interact in the two-hybrid system. Using the yeast two-hybrid system, we have characterized Upf1p-Nmd2p and Nmd2p-Upf3p interactions (see above and references 12 and 14). We were also interested in determining whether Upf1p-Upf3p interactions could be detected with this system, and we used two sets of constructs to test this possibility. In one experiment, we assayed the ability of a full-length *lexA*(DB)-*UPF3* fusion to interact with a panel of *GAL4*(AD)-*UPF1* fusions (Fig. 3, constructs 1 to 14). When coexpressed with *lexA*(DB)-*UPF3*, all of the *GAL4*(AD)-*UPF1* fusions that are capable of interacting with *GAL4*(DB)-*NMD2*(933–1089) yielded detectable levels of β-galactosidase activity (Fig. 3, constructs 1 to 7 and 9 to 11). Of these, the highest levels of activity were observed with *GAL4*(AD) fusions containing *UPF1* fragments from residues 1 to 666, 1 to 207, and 62 to 207 (Fig. 3, constructs 2, 6, and 10). All of the *GAL4*(AD)-*UPF1* fusions that are not capable of interacting with *GAL4*(DB)-*NMD2*(933–1089) yielded only background levels of β-galactosidase activity (Fig. 3, constructs 8 and 12 to 14). These results suggest that Upf1p and Upf3p do interact in this assay

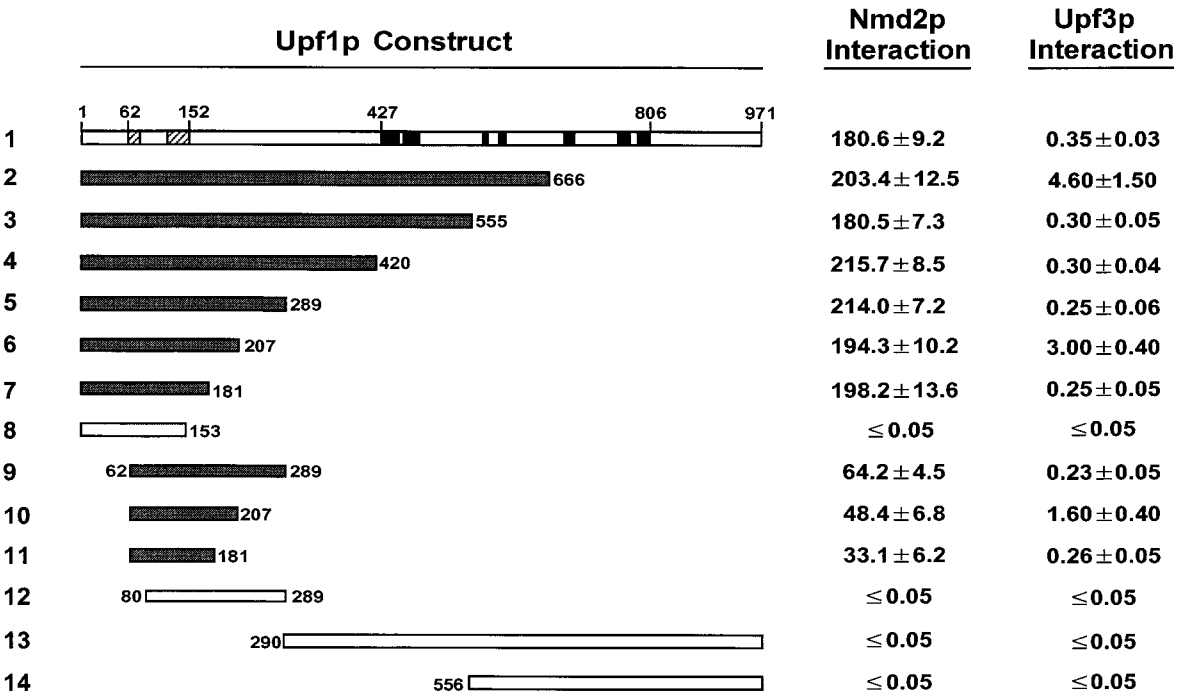

FIG. 3. Identification of Nmd2p- and Upf3p-interacting domains within Upf1p. The yeast two-hybrid system was used to identify Nmd2p- and Upf3p-interacting domains within Upf1p. To test for interaction between Upf1p and Nmd2p, a *GAL4*(DB)-*NMD2*(933–1089) fusion that contains the entire Upf1p-interacting domain of Nmd2p was cotransformed into the tester strain GGY1::171 with each of 14 *GAL4*(AD)-*UPF1* fusions encoding distinct fragments of Upf1p. To test for interactions between Upf1p and Upf3p, a *lexA*(DB)-*UPF3*(1–387) fusion was cotransformed with each of 14 *GAL4*(AD)-*UPF1* fusions into strain L40. Individual transformants were selected, and β-galactosidase activity was determined quantitatively in a liquid assay. *UPF1* sequences fused to the *GAL4*(AD) are illustrated. The hatched boxes and black boxes shown in construct 1 represent the two putative Zn^{2+} fingers and seven conserved motifs common to the members of helicase superfamily I, respectively (1, 18, 22). The grey and open boxes in constructs 2 to 14 represent *GAL4*(AD)-*UPF1* fusions that, respectively, do or do not interact with Nmd2p and Upf3p. Interaction values depict mean β-galactosidase activities ± standard deviations for at least three independent assays performed on cultures derived from individual colonies.

and that the Upf3p- and Nmd2p-interacting domains within Upf1p overlap or are identical to each other.

We also tested the ability of the full-length *GAL4*(AD)-*UPF1* fusion to interact with a panel of *lexA*(DB)-*UPF3* fusions (Fig. 2, constructs 1 to 15). When coexpressed with full-length *GAL4*(AD)-*UPF1*, all but two of the *lexA*(DB)-*UPF3* fusions that are capable of interacting with *GAL4*(AD)-*NMD2*(564–1089) accumulated β-galactosidase activity, although to considerably lesser extents (Fig. 2, constructs 1 to 4, 7, 10, 11, and 13); all of the *lexA*(DB)-*UPF3* fusions that do not interact with *GAL4*(AD)-*NMD2*(564–1089) yielded background levels of β-galactosidase activity (Fig. 2, constructs 5, 6, 9, 12, and 15). These results indicate that Upf1- and Nmd2p-interacting domains within Upf3p also overlap or are identical to each other.

Two-hybrid interactions of Upf1p-Nmd2p, Nmd2p-Upf3p, and Upf1p-Upf3p in the absence of genomic *UPF1*, *NMD2*, or *UPF3*. The two-hybrid approach does not distinguish between direct and indirect interactions. For example, Upf3p could associate with Upf1p by using Nmd2p as a bridging molecule. We therefore repeated a subset of the previous two-hybrid assays with isogenic strains with *UPF1*, *NMD2*, or *UPF3* individually deleted. Upf1p-Nmd2p and Nmd2p-Upf3p interactions were tested with the *GAL4*(AD)-*UPF1*(1–971)/*lexA*(DB)-*NMD2*^{DN}(326–1089) and *lexA*(DB)-*NMD2*^{DN}(326–1089)/*GAL4*(AD)-*UPF3*(1–387) fusion pairs, respectively. Interactions between Upf1p and Upf3p were tested with both a weakly interacting pair of fusion proteins [*lexA*(DB)-*UPF3*(1–387)/*GAL4*(AD)-*UPF1*(1–971)] and a more effectively interacting pair [*lexA*(DB)-*UPF3*(1–387)/*GAL4*(AD)-*UPF1*(1–207). These experiments showed that in *upf1*Δ and *upf3*Δ strains, all of the tested interactions occur as well as they do in wild-type cells (Table 5), indicating that they do not require the *UPF1* and *UPF3* gene products. Likewise, deletion of the *NMD2* gene had no effect on Upf1p-Nmd2p or Nmd2p-Upf3p interactions (Table 5). However, *nmd2*Δ cells were completely incapable of supporting either pair of Upf1p-Upf3p interactions (Tables 5 and 6). These results imply that Nmd2p can bind Upf1p and

TABLE 5. Upf1p-Nmd2p, Nmd2p-Upf3p, and Upf1p-Upf3p two-hybrid interactions in the absence of genomic *UPF1 NMD2*, or *UPF3*[a]

Strain	β-Galactosidase activity for the following interaction (bait-prey)		
	Upf1p-Nmd2p	Nmd2p-Upf3p	Upf3p-Upf1p
Wild type	+	+	+
*upf1*Δ	+	+	+
*nmd2*Δ	+	+	−
*upf3*Δ	+	+	+

[a] The construction of tester strains containing single deletions of *UPF1*, *NMD2*, and *UPF3* is described in Materials and Methods. The fusion constructs *lexA*(DB)-*NMD2*^{DN}(326–1089)/*GAL4*(AD)-*UPF1*(1–971) and *lexA*(DB)-*NMD2*^{DN}(326–1089)/*GAL4*(AD)-*UPF3*(1–387) were used to examine interactions between Upf1p and Nmd2p and between Nmd2p and Upf3p, respectively. Constructs encoding the fusion pairs *lexA*(DB)-*UPF3*(1–387)/*GAL4*(AD)-*UPF1*(1–971) (weak interactors) and *lexA*(DB)-*UPF3*(1–387)/*GAL4*(AD)-*UPF1*(1–207) (moderately strong interactors) were used to examine interactions between Upf1p and Upf3p. β-Galactosidase activity was determined qualitatively by replica plating on X-Gal-containing plates. +, blue color development; −, no color development (after 7 days of incubation at 30°C).

TABLE 6. Overexpression of *NMD2* enhances two-hybrid interaction between Upf1p and Upf3p[a]

Strain	β-Galactosidase activity (U) for:	
	lexA-UPF3(1–387)/*GAL4*(AD)-*UPF1*(1-971)	*lexA-UPF3*(1-387)/*GAL4*(AD)-*UPF1*(1-207)
NMD2	0.35 ± 0.03	3.00 ± 0.40
NMD2[*NMD2*]	3.10 ± 0.30	33.60 ± 3.90
NMD2[*NMD2*^{DN}]	43.30 ± 3.00	69.30 ± 5.70
NMD2[*NMD2-CΔ166*]	0.30 ± 0.04	3.50 ± 0.80
NMD2[*NMD2-CΔ526*]	0.30 ± 0.05	2.70 ± 0.30
nmd2Δ	≤0.05	≤0.05

[a] Two-hybrid interaction between Upf1p and Upf3p was assayed in strains overexpressing the *NMD2* gene or fragments of *NMD2*. Constructs expressing *lexA*(DB)-*UPF3*(1–387)/*GAL4*(AD)-*UPF1*(1–971) (weak interactors) and *lexA*(DB)-*UPF3*(1–387)/*GAL4*(AD)-*UPF1*(1–207) (moderately strong interactors) were tested. *NMD2*[*NMD2*], strain overexpressing full-length *NMD2*; *NMD2*[*NMD2*^{DN}], strain overexpressing the original dominant-negative fragment encoding Nmd2p residues 326 to 1089; *NMD2*[*NMD2-CΔ166*], strain overexpressing *NMD2-CΔ166*, a construct that encodes a 166-amino-acid deletion from the Nmd2p C terminus; *NMD2*[*NMD2-CΔ526*], strain overexpressing *NMD2-CΔ526*, a construct that encodes a 526-amino-acid deletion from the Nmd2p C terminus. *NMD2* and its derivatives contain N-terminal triple-HA tags, and their expression was driven by the *ADH1* promoter on a centromere-based vector, pRS313. Individual transformants were selected, and β-galactosidase activity was determined quantitatively in a liquid assay. β-Galactosidase activities from wild-type (*NMD2*) and *nmd2*Δ strains are also shown. Values represent the means ± standard deviations for at least three independent assays performed on cultures derived from individual colonies.

Upf3p simultaneously and promote the formation of a Upf1p-Nmd2p-Upf3p complex in vivo.

Overexpression of Nmd2p enhances the formation of a Upf1p-Nmd2p-Upf3p complex. The data described above suggest that Nmd2p bridges the apparent interaction between Upf1p and Upf3p. To test this hypothesis further, we asked whether overexpression of Nmd2p could alter the extent of the Upf1p-Upf3p two-hybrid interaction. A series of plasmids expressing either full-length Nmd2p or fragments thereof were introduced into yeast cells coexpressing either of two pairs of fusion proteins, *lexA*(DB)-*UPF3*(1–387)/*GAL4*(AD)-*UPF1*(1–971) or *lexA*(DB)-*UPF3*(1–387)/*GAL4*(AD)-*UPF1*(1–207). In the wild-type *NMD2* background, the level of β-galactosidase activity was low for both pairs of interactors (although significantly better for the pair including truncated Upf1p) (Table 6). However, when full-length *NMD2*, or a fragment of *NMD2* including residues 564 to 1089, was overexpressed, yeast strains containing both pairs of interactors showed approximately 10- to 100-fold increases in β-galactosidase activity. In contrast, overexpression of Nmd2p fragments that contain deletions of either the Upf1p-interacting domain (*NMD2-CΔ166*) or both the Upf1p- and Upf3p-interacting domains (*NMD2-CΔ526*) had no effect on the level of β-galactosidase activity (Table 6). These data indicate that overexpression of Nmd2p can enhance the formation of a Upf1p-Nmd2p-Upf3p complex in vivo and that this activity is dependent on the presence of intact Upf1p- and Upf3p-interacting domains within Nmd2p.

We also introduced a plasmid overexpressing a fragment of Nmd2p from residues 564 to 1089 into yeast strains containing the *GAL4*(AD)-*UPF1*(1–971) fusion and each of a panel of *lexA*(DB)-*UPF3* fusions (Fig. 2, constructs 1 to 15). As shown in Fig. 2, levels of β-galactosidase activity were significantly increased in yeast strains expressing *lexA*(DB)-*UPF3* fusion proteins previously shown to be capable of interacting with Nmd2p (Fig. 2, constructs 1 to 4, 7, 8, 10, 11, 13, and 14). However, levels of β-galactosidase activity were not increased in yeast strains expressing *lexA*(DB)-*UPF3* fusion proteins previously shown to be incapable of interacting with Nmd2p (Fig. 2, constructs 5, 6, 9, 12, and 15). This indicates that the formation of a Upf1p-Nmd2p-Upf3p complex is also dependent on the ability of Upf3p to interact with Nmd2p. Comparable experiments showed that *UPF1* deletions that disrupt of the ability of Upf1p to interact with Nmd2p also abolish complex formation (data not shown). Collectively, these results reinforce the conclusion that Nmd2p is a bridging molecule and that the two-hybrid Upf1p-Upf3p interaction must be indirect.

Single or multiple deletions of *UPF1*, *NMD2*, and *UPF3* inhibit nonsense-mediated mRNA decay to the same extent. The results of our two-hybrid analyses (see above and references 12 and 14) strongly suggest that Upf1p, Nmd2p, and Upf3p function either as a complex or in closely related steps of the nonsense-mediated mRNA decay pathway. This conclusion was strengthened by analyzing the nonsense-mediated mRNA decay phenotypes associated with single or multiple deletions of the genes encoding each of these proteins. To this end, we constructed yeast strains containing either single deletions of *UPF1*, *NMD2*, and *UPF3*, double deletions of *UPF1*/*NMD2*, *NMD2*/*UPF3*, and *UPF1*/*UPF3*, or a triple deletion of all three genes (see Materials and Methods). Total RNA was isolated from yeast strains containing these deletions, and Northern blot analysis was used to monitor the levels of the *CYH2* pre-mRNA, an endogenous nonsense-containing mRNA (12, 13). Northern analysis demonstrated that the abundance of the *CYH2* pre-mRNA increased to equal extents in strains carrying the single deletions, the double deletions, or the triple deletion (Fig. 4).

Both the N-terminal Upf3p-binding site and a region including residues 772 to 816 of Nmd2p are required for dominant inhibition of nonsense-mediated mRNA decay. We have previously shown that overexpression of a *GAL4*(AD) fusion to a 764-amino-acid C-terminal fragment of Nmd2p can inhibit the nonsense-mediated mRNA decay pathway in a dominant manner when the fusion protein is localized to the cytoplasm but not when it is localized to the nucleus (12). Recently, we demonstrated that the dominant-negative effects of this *nmd2* allele are independent of its Upf1p-binding activity, since a deletion of the entire Upf1p-interacting domain of Nmd2p had no effect on the inhibition of mRNA decay (14). To determine the region(s) responsible for the dominant-negative effects, we examined the inhibitory activity of the panel of *NMD2* fragments shown in Fig. 1A. Each of these fragments was cloned into an expression vector and overexpressed in an *NMD2* wild-type strain as described previously (14). Northern blot analysis of the relative levels of the *CYH2* pre-mRNA and mRNA was used to monitor the activity of the nonsense-mediated mRNA decay pathway in each of the transformants. As shown in Fig. 1A and C, N-terminal deletions of Nmd2p up to residue 563 have no significant effects on dominant-negative activity (constructs 1 to 3). However, N-terminal deletions extending to residue 771 lead to a complete loss of inhibitory activity (Fig. 1A and C constructs 4 to 6), indicating that the region spanning residues 564 to 771 is required for dominant inhibition. *NMD2* fragments containing C-terminal deletions up to residue 816 still inactivated nonsense-mediated mRNA decay as efficiently as the original dominant-negative *nmd2* allele (Fig. 1A and C, compare construct 1 to constructs 10 to 12 and 18 to 20), indicating that the region from residue 817 to 1089, which includes the entire acidic domain and the entire Upf1p-interacting domain of Nmd2p, is not required for dominant inhibition. In contrast, further C-terminal deletions up to Nmd2p residue 771 lead to a complete loss of inhibitory activity (Fig. 1A and C, constructs 13, 14, 21, and 22), indicating that the

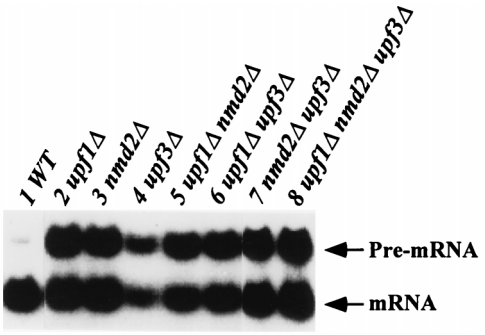

Strain	*CYH2* pre-mRNA/mRNA
1	0.12
2	1.00
3	0.98
4	0.97
5	1.10
6	1.05
7	1.05
8	1.10

FIG. 4. Single or multiple deletions of *UPF1*, *NMD2*, and *UPF3* have identical nonsense-mediated mRNA decay phenotypes. Total RNA was isolated from yeast cells containing single or multiple deletions of *UPF1*, *NMD2*, and *UPF3*. The construction of these strains is described in Materials and Methods. Northern blotting was performed as described in the legend to Fig. 1. *CYH2* pre-mRNA/mRNA ratios from these cells are summarized. WT, wild type.

region from residue 772 to 816 is also required for dominant inhibition.

Although residues 564 to 771 and 772 to 816 are required for dominant inhibition, overexpression of *NMD2* fragments containing either region alone is not sufficient to inactivate nonsense-mediated mRNA decay (Fig. 1A and C, constructs 6 and 22). Because the *NMD2* fragment containing both regions can inactivate nonsense-mediated mRNA decay efficiently (Fig. 1A and C, construct 20), we conclude that the Nmd2p domain encompassing residues 564 to 816 is responsible for the dominant-negative effect. Interestingly, this region spans residues that are required (residues 564 to 771) as well as residues that are not required (residues 772 to 816) for Nmd2p binding to Upf3p (see above).

Overexpression of Upf3p alone is not sufficient to alleviate the dominant-negative effects of Nmd2^{DN}p. Since the minimal dominant-negative fragment of Nmd2p includes a Upf3p-binding site (see above), it is formally possible that the dominant-negative effect is attributable to the saturation of functional Upf3p with nonfunctional Nmd2p. To test this possibility, we transformed a series of plasmids expressing *UPF3* or epitope-tagged *UPF3* into yeast cells containing a dominant-negative *nmd2* allele. The results of these experiments are shown in Fig. 5. In cells containing the dominant-negative *nmd2* allele, expression of *UPF3* from a single-copy or a high-copy-number plasmid had no effect on dominant-negative inhibition (Fig. 5B, lanes 3 and 4). Furthermore, there was no effect on dominant inhibition when Upf3p expression from a high-copy-number plasmid was enhanced by replacing the normal *UPF3* promoter with the more potent *ADH1* promoter (Fig. 5B, lanes 5 and 6). In contrast, expression of *NMD2* from a single-copy or a high-copy-number plasmid or expression of HA-*NMD2* from the *ADH1* promoter on a high-copy-number plasmid led to a dosage-dependent increase of nonsense-mediated mRNA decay activity (Fig. 5A, lanes 3 to 5). These results indicate that the dominant-negative effect of Nmd2p is targeted to another interacting component that is distinct from Upf3p.

DISCUSSION

Nonsense-mediated mRNA decay is dependent on the activity of the interacting components Upf1p, Nmd2p, and Upf3p. *UPF1*, *NMD2*/*UPF2*, and *UPF3* are the three principal nonessential genes whose products have been shown to be required for the selective decay of only those transcripts in *S. cerevisiae* that contain premature translational termination codons (for a review, see reference 16). While structural and biochemical analyses suggest that Upf1p may be an RNA-binding protein with ATPase and RNA helicase activities (1, 7, 18, 22), little else is known about the functions of these factors. As an approach to elucidating their respective roles in mRNA decay, we have begun to identify the proteins with which these factors interact and to define the relevant interacting domains. Thus, in earlier studies, we showed that Upf1p and Nmd2p are interacting proteins, localized the Upf1p-interacting domain of Nmd2p to its 157-amino-acid C terminus, demonstrated that interaction between Upf1p and Nmd2p is required for nonsense-mediated mRNA decay, and established that at least one other factor must interact with Nmd2p (12, 14). Here, we sought to identify the other factor(s) and used the yeast two-hybrid system to show that both *UPF1* and *UPF3* encode Nmd2p-interacting proteins and that *NMD2* encodes a Upf3p-interacting protein (12a). Interactions between Nmd2p and Upf3p have also been reported recently (37). Further evidence for these interactions was provided by experiments that defined specific Nmd2p-interacting domains within Upf1p and Upf3p and specific Upf1p- and Upf3p-interacting domains within Nmd2p (Fig. 1 to 3), as well as by experiments which showed that cells harboring single or multiple deletions of *UPF1*, *NMD2*, and *UPF3* inhibit nonsense-mediated mRNA decay to the same extent (Fig. 4) (5, 12, 19). Collectively, these data demonstrate that Upf1p, Nmd2p, and Upf3p are interacting components of the yeast nonsense-mediated mRNA decay pathway.

Two-hybrid interactions between Upf1p and Upf3p are indirect and are bridged by Nmd2p. Our two-hybrid analyses identified Upf1p-Nmd2p, Nmd2p-Upf3p, and Upf1p-Upf3p interactions (Fig. 1 to 3) (12, 14). To determine whether the observed pairwise interactions require the respective third components, we examined the consequences that deleting genomic copies of *UPF1*, *NMD2*, and *UPF3* had on the outcome of two-hybrid experiments. We find that single deletion of *UPF1*, *NMD2*, or *UPF3* has no effect on Upf1p-Nmd2p or Nmd2p-Upf3p interactions, indicating that they occur without the participation of the absent factor (Table 5). However, deletion of *NMD2* completely abolishes the apparent interaction between Upf1p and Upf3p (Tables 5 and 6), indicating that this interaction in wild-type cells is indirect and is bridged by Nmd2p. Further evidence for this conclusion includes the

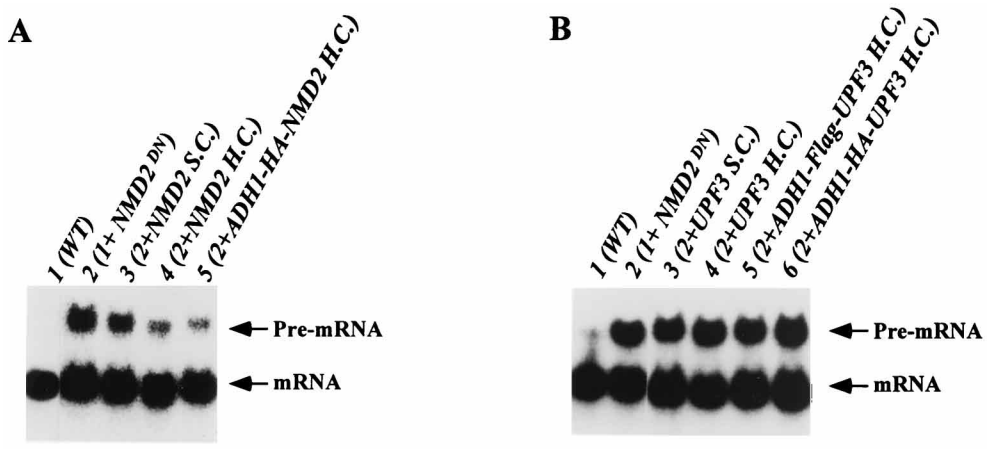

Strain	*CYH2* pre-mRNA/mRNA
1	0.12
2	0.50
3	0.30
4	0.18
5	0.18

Strain	*CYH2* pre-mRNA/mRNA
1	0.12
2	0.50
3	0.55
4	0.50
5	0.55
6	0.50

FIG. 5. Overexpression of *NMD2*, but not *UPF3*, can alleviate the dominant-negative effects of Nmd2^{DN}p. (A) Overexpression of *NMD2* alleviates, in a dosage-dependent manner, the inhibition of mRNA decay caused by a dominant-negative allele of *NMD2*. Plasmids expressing a wild-type (WT) or HA-tagged *NMD2* gene were transformed into yeast cells expressing the dominant-negative allele of *NMD2*. Total RNA was isolated from these cells, and Northern blotting was performed as described in the legend to Fig. 1. Lane 1, RNA from HFY1200 harboring pACTII(ΔNLS) only; lane 2, HFY1200 harboring pACTII-*NMD2*^{DN}; lane 3, HFY1200 harboring pACTII-*NMD2*^{DN} and pRS314-*NMD2*; lane 4, HFY1200 harboring pACTII-*NMD2*^{DN} and YEplac112-*NMD2*; lane 5, HFY1200 harboring pACTII-*NMD2*^{DN} and YEplac112-*ADH1*p-HA-*NMD2*. *CYH2* pre-mRNA/mRNA ratios from these cells are summarized below the blot. (B) Overexpression of *UPF3* cannot alleviate the inhibition of mRNA decay caused by a dominant-negative allele of *NMD2*. Plasmids expressing wild-type or epitope-tagged *UPF3* genes were individually transformed into yeast cells expressing the dominant-negative allele of *NMD2*. Total RNA was isolated from these cells, and Northern blotting was performed as described in the legend to Fig. 1. Lane 1, RNA from HFY1200 harboring pACTII(ΔNLS) only; lane 2, HFY1200 harboring pACTII-*NMD2*^{DN}; lane 3, HFY1200 harboring pACTII-*NMD2*^{DN} and pRS314-*UPF3*; lane 4, HFY1200 harboring pACTII-*NMD2*^{DN} and YEplac112-*UPF3*; lane 5, HFY1200 harboring pACTII-*NMD2*^{DN} and YEplac112-*ADH1*p-FLAG-*UPF3*; lane 6, HFY1200 harboring pACTII-*NMD2*^{DN} and YEplac112-*ADH1*p-HA-*UPF3*. *CYH2* pre-mRNA/mRNA ratios from these cells are summarized below the blot. S.C., single copy; H.C., high copy.

following: (i) overexpression of either full-length Nmd2p or its dominant-negative fragment enhances the apparent interaction of Upf1p and Upf3p by 10- to 200-fold (Table 6 and Fig. 2); (ii) this enhancement is dependent on the presence of intact Upf1p- and Upf3p-interacting domains within Nmd2p and on the ability of Upf1p and Upf3p to interact with Nmd2p (Table 6 and Fig. 2 and data not shown); (iii) the domains of Upf1p and Upf3p putatively involved in the interaction with each other correspond to the domains on the two proteins which interact with Nmd2p (Fig. 2 and 3); and (iv) a two-hybrid screen with Upf1p as bait failed to identify Upf3p as a Upf1p-interacting protein, and a two-hybrid screen with Upf3p as bait failed to identify Upf1p as a Upf3p-interacting protein, but both screens identified Nmd2p an interacting partner (12, 12a). The fact that Nmd2p is required for the observed interaction between Upf1p and Upf3p indicates that Nmd2p can interact with both Upf1p and Upf3p simultaneously and that it may promote the formation of a Upf1p-Nmd2p-Upf3p complex in vivo. Experiments demonstrating that all three proteins are predominantly localized to the cytoplasm support this possibility (3, 12b, 26), but coimmunoprecipitation or cross-linking experiments are necessary for definitive identification of such a complex.

When assaying the two-hybrid interactions between Upf1p and Upf3p in *NMD2* wild-type cells, we observed that a subset of truncations in either Upf1p or Upf3p led to a significant increase of β-galactosidase activity (Fig. 2, constructs 2, 3, 7, 10, and 11; Fig. 3, constructs 2, 6, and 10). Each of these Upf1p or Upf3p fragments led to considerably more β-galactosidase activity than the respective full-length polypeptide. Such increases may simply reflect the loss of polypeptide sequences that interfere with two-hybrid interactions (e.g., masking domains or possible cytoplasmic retention signals), or they may indicate that binding of these Upf1p or Upf3p fragments to Nmd2p results in a conformational change in Nmd2p that, in turn, promotes increased binding of Nmd2p to Upf3p or Upf1p. The enhancement of Upf3p interaction by some N-terminal deletions of Nmd2p may be attributable to similar effects (Fig. 1, constructs 3 and 18).

Novelty of the protein domains involved in Upf1p-Nmd2p and Nmd2p-Upf3p interactions. To delineate the domains essential for Upf1p-Nmd2p and Nmd2p-Upf3p interactions, we

used qualitative and quantitative two-hybrid analysis of deletion mutants of the respective genes. These experiments indicate the following. (i) None of the interacting domains identified in this study has significant sequence homology with known protein-protein interaction motifs, except for the Nmd2p-interacting domain of Upf1p and a weaker Upf3p-interacting domain of Nmd2p (see below). They may thus represent new classes of such structures. (ii) Upf1p and Upf3p interact with distinct domains of Nmd2p. The Upf1p-interacting domain of Nmd2p was previously mapped to a 157-amino-acid segment at its C terminus in which two regions, spanning residues 947 to 985 and 1034 to 1061, appear to be the principal Upf1p-interacting epitopes (14). The major Upf3p-interacting domain is located within Nmd2p residues 564 to 771, and a weaker domain is localized to a region from residue 879 to 933. The latter domain, which includes almost all of the hyperacidic domain of Nmd2p (12), enhances binding to Upf3p (Fig. 1A, constructs 10 and 18) but also appears to inhibit interaction with Upf1p (14). Hyperacidic domains have been found in a number of other proteins, such as nucleolins and transcription factors, and their functions are largely unknown (17). If the hyperacidic domain is actually involved in regulating Nmd2p-Upf3p interaction, it is likely to do so via interaction with a region of clustered positive charge in Upf3p. In this regard, it should be noted that in a two-hybrid assay for interaction with the hyperacidic domain of Nmd2p, the C-terminal 256-amino-acid segment of Upf3p, which contains multiple lysine-argine-rich regions (19), yielded the same level of β-galactosidase activity as did full-length Upf3p (data not shown). (iii) The Zn^{2+} finger-like motifs of Upf1p, encompassed within residues 62 to 152 (1, 22), are necessary but not sufficient for interaction with Nmd2p. Deletion analysis indicates that residues 62 to 181, which include the two Zn^{2+} finger motifs and a short flanking region, comprise the minimal domain sufficient for interaction with Nmd2p (Fig. 3). Although Zn^{2+} finger motifs in other proteins have been implicated in both DNA and RNA binding (4), our results indicate that these motifs are also involved in both heterodimerization with Nmd2p (see above) and homodimerization (12a). This region of Upf1p, like that recently identified in the *RAG1* protein (29), thus may represent a structure that is distinct from that of the classical Zn^{2+} finger motif and may exemplify a new class of protein-protein interaction domains.

Dominant-negative Nmd2p targets a factor other than Upf1p or Upf3p. Overexpression of a protein comprised of a 764-amino-acid C-terminal fragment of Nmd2p fused to the *GAL4*(AD) has a dominant-negative effect on nonsense-mediated mRNA decay when the protein is localized in the cytoplasm but not when it is localized in the nucleus (12). Since deletion or point mutations in the Upf1p-interacting domain of this fragment, or overexpression of Upf1p, do not alter dominant-negative inhibition, we have concluded that the inhibitory effects on mRNA decay arise from Nmd2p interaction with a factor other than Upf1p (14). Further deletion mapping has shown that two regions of Nmd2p, spanning residues 564 to 771 and 772 to 816, are required for dominant-negative activity and that neither domain alone is sufficient for such activity (Fig. 1A and C). Because these regions essential to the dominant-negative activity of Nmd2p include the principal Upf3p-interacting domain (Fig. 1A), it is formally possible that the dominant-negative effect is attributable to the saturation of functional Upf3p with nonfunctional Nmd2p. However, two observations indicate that the dominant-negative fragment of Nmd2p must target a factor other than Upf3p: (i) overexpression of Upf3p does not reverse the dominant inhibition (Fig. 5), and (ii) there is no correlation between the efficiency with which Nmd2p fragments bind Upf3p in the two-hybrid assay and the extent of dominant-negative inhibition by the same fragments (Fig. 1).

The simplest explanation for these observations is that both the principal Upf3p-interacting domain (residues 564 to 771) and the region from residue 772 to 816 may contribute to the binding of yet another factor and that overexpression of the dominant-negative Nmd2p fragment leads to titration of only that unidentified factor. Alternative explanations include the possibility that the region from residue 772 to 816 is part of the binding site for a novel factor and that both this factor and Upf3p are simultaneously titrated by overexpression of dominant-negative Nmd2p. A variation on the latter hypothesis suggests that binding of the novel factor to Nmd2p may require the presence of Upf3p. Clearly, further characterization of the genes identified in the two-hybrid screen in which the *nmd2* dominant-negative fragment was used as bait may help to elucidate the mechanism in question.

ACKNOWLEDGMENTS

This work was supported by a grant (GM27757) to A.J. from the National Institutes of Health and by a postdoctoral fellowship to F.H. from the Charles A. King Trust, Fleet Bank, Boston, Mass.

We thank Stan Fields, Paul Bartel, Stephen Elledge, David Mangus, Stan Hollenberg, Elizabeth Craig, and Philip James for plasmids and strains and Dorit Zuk for helpful comments on the manuscript.

REFERENCES

1. **Altamura, N., O. Groudinsky, G. Dujardin, and P. P. Slonimski.** 1992. *NAM7* nuclear gene encodes a novel member of a family of helicases with a Zn-ligand motif and is involved in mitochondrial functions in *Saccharomyces cerevisiae*. J. Mol. Biol. **224:**575–587.
2. **Altschul, S. F., W. Gish, W. Miller, E. W. Myers, and D. J. Lipman.** 1990. Basic local alignment search tool. J. Mol. Biol. **215:**403–410.
3. **Atkin, A. L., N. Altamura, P. Leeds, and M. R. Culbertson.** 1995. The majority of yeast *UPF1* co-localizes with polyribosomes in the cytoplasm. Mol. Biol. Cell **6:**611–625.
4. **Berg, J. M.** 1993. Zinc-finger proteins. Curr. Opin. Struct. Biol. **3:**11–16.
5. **Cui, Y., K. W. Hagan, S. Zhang, and S. W. Peltz.** 1995. Identification and characterization of genes that are required for the accelerated degradation of mRNAs containing a premature translational termination codon. Genes Dev. **9:**423–436.
6. **Culbertson, M. R., K. M. Underbrink, and G. R. Fink.** 1980. Frameshift suppression in *Saccharomyces cerevisiae*. II. Genetic properties of group II suppressors. Genetics **95:**833–853.
7. **Czaplinski, K., Y. Weng, K. W. Hagan, and S. W. Peltz.** 1995. Purification and characterization of the Upf1 protein: a factor involved in translation and mRNA degradation. RNA **1:**610–623.
8. **Dinman, J. D., and R. B. Wickner.** 1994. Translational maintenance of frame: mutants of *Saccharomyces cerevisiae* with altered −1 ribosomal frameshifting efficiencies. Genetics **136:**75–86.
9. **Durfee, T., K. Becherer, P. L. Chen, S. H. Yeh, Y. Yang, A. E. Kilburn, W. H. Lee, and S. J. Elledge.** 1993. The retinoblastoma protein associates with the protein phosphatase type 1 catalytic subunit. Genes Dev. **7:**555–569.
10. **Fields, S., and O.-K. Song.** 1989. A novel genetic system to detect protein-protein interactions. Nature **340:**245–246.

10a. **Ganesan, R., F. He, and A. Jacobson.** Unpublished data.

11. **Gietz, R. D., and A. Sugino.** 1988. New yeast-*Escherichia coli* shuttle vectors constructed with in vitro mutagenized yeast genes lacking six-base pair restriction sites. Gene **74:**527–534.
12. **He, F., and A. Jacobson.** 1995. Identification of a novel component of the nonsense-mediated mRNA decay pathway by use of an interacting protein screen. Genes Dev. **9:**437–454.

12a. **He, F., and A. Jacobson.** Unpublished data.

12b. **He, F., D. Mangus, A. H. Brown, D. Zuk, and A. Jacobson.** Unpublished data.

13. **He, F., S. W. Peltz, J. L. Donahue, M. Rosbash, and A. Jacobson.** 1993. Stabilization and ribosome association of unspliced pre-mRNAs in a yeast *upf1*$^-$ mutant. Proc. Natl. Acad. Sci. USA **90:**7034–7039.
14. **He, F., A. H. Brown, and A. Jacobson.** 1996. Interaction between Nmd2p and Upf1p is required for activity but not for dominant-negative inhibition of the nonsense-mediated mRNA decay pathway in yeast. RNA **2:**153–170.
15. **Hollenberg, S. M., R. Sternglanz, P. F. Cheng, and H. Weintraub.** 1995. Identification of a new family of tissue-specific basic helix-loop-helix proteins with a two-hybrid system. Mol. Cell. Biol. **15:**3813–3822.
16. **Jacobson, A., and S. W. Peltz.** 1996. Interrelationships of the pathways of

mRNA decay and translation in eukaryotic cells. Annu. Rev. Biochem. **65:**693–739.
17. **Karlin, S.** 1995. Statistical significance of sequence patterns in proteins. Curr. Opin. Struct. Biol. **5:**360–371.
18. **Koonin, E. V.** 1992. A new group of putative RNA helicases. Trends Biochem. Sci. **17:**495–497.
19. **Lee, B.-S., and M. R. Culbertson.** 1995. Identification of an additional gene required for eukaryotic nonsense mRNA turnover. Proc. Natl. Acad. Sci. USA **92:**10354–10358.
20. **Lee, S. I., J. G. Umen, and H. E. Varmus.** 1995. A genetic screen identifies cellular factors involved in retroviral −1 frameshifting. Proc. Natl. Acad. Sci. USA **92:**6587–6591.
21. **Leeds, P., S. W. Peltz, A. Jacobson, and M. R. Culbertson.** 1991. The product of the yeast *UPF1* gene is required for rapid turnover of mRNAs containing a premature translational termination codon. Genes Dev. **5:**2303–2314.
22. **Leeds, P., J. M. Wood, B.-S. Lee, and M. R. Culbertson.** 1992. Gene products that promote mRNA turnover in *Saccharomyces cerevisiae*. Mol. Cell. Biol. **12:**2165–2177.
23. **Maddock, J. R., E. M. Weidenhammer, C. C. Adams, R. L. Lunz, and J. L. Woolford.** 1994. Extragenic suppressors of *Saccharomyces cerevisiae prp4* mutations identify a negative regulator of *PRP* genes. Genetics **136:**833–847.
24. **Miller, J. H.** 1972. Experiments in molecular genetics. Cold Spring Harbor Laboratory Press, Cold Spring Harbor, N.Y.
25. **Peltz, S. W., A. H. Brown, and A. Jacobson.** 1993. mRNA destabilization triggered by premature translational termination depends on at least three *cis*-acting sequence elements and one *trans*-acting factor. Genes Dev. **7:**1737–1754.
26. **Peltz, S. W., C. Trotta, F. He, A. Brown, J. Donahue, E. Welch, and A. Jacobson.** 1993. Identification of the *cis*-acting sequences and *trans*-acting factors involved in nonsense-mediated mRNA decay, vol. H71, p. 1–10. *In* M. Tuite, J. McCarthy, A. Brown, and F. Sherman (ed.), Protein synthesis and targetting in yeast. Springer-Verlag, New York, N.Y.
27. **Peltz, S. W., F. He, E. Welch, and A. Jacobson.** 1994. Nonsense-mediated mRNA decay in yeast. Prog. Nucleic Acids Res. Mol. Biol. **47:**271–297.
28. **Pinto, I., J. G. Na, F. Sherman, and M. Hampsey.** 1992. *cis*- and *trans*-acting suppressors of a translation initiation defect at the *cyc1* locus of *Saccharomyces cerevisiae*. Genetics **132:**97–112.
29. **Rodgers, K. K., Z. Bu, K. G. Fleming, D. G. Schatz, D. M. Engelman, and J. E. Coleman.** 1996. A zinc-binding domain involved in the dimerization of RAG1. J. Mol. Biol. **260:**70–84.
30. **Rose, M. D., F. Winston, and P. Hieter.** 1990. Methods in yeast genetics: a laboratory course manual. Cold Spring Harbor Laboratory, Cold Spring Harbor, N.Y.
31. **Rothstein, R.** 1991. Targeting, disruption, replacement, and allele rescue: integrative DNA transformation in yeast. Methods Enzymol. **194:**281–301.
32. **Sambrook, J., E. F. Fritsch, and T. Maniatis.** 1989. Molecular cloning: a laboratory manual. Cold Spring Harbor Laboratory Press, Cold Spring Harbor, N.Y.
33. **Sanger, F., S. Nicklen, and A. R. Coulson.** 1977. DNA sequencing with chain-terminating inhibitors. Proc. Natl. Acad. Sci. USA **74:**5463–5467.
34. **Schiestl, R. H., and R. D. Gietz.** 1989. High efficiency transformation of intact yeast cells using single stranded nucleic acids as a carrier. Curr. Genet. **16:**339–346.
35. **Sikorski, R. S., and P. Hieter.** 1989. A system of shuttle vectors and yeast host strains designated for efficient manipulation of DNA in *Saccharomyces cerevisiae*. Genetics **122:**19–27.
36. **Thompson, E. A., and G. S. Roeder.** 1989. Expression and DNA sequence of *RED1*, a gene required for meiosis I chromosome segregation in yeast. Mol. Gen. Genet. **218:**293–301.
37. **Weng, Y., K. Czaplinski, and S. W. Peltz.** 1996. Identification and characterization of mutations in the *UPF1* gene that affect nonsense suppression and the formation of the Upf protein complex but not mRNA turnover. Mol. Cell. Biol. **16:**5491–5506.
38. **White, T. J., N. Arnheim, and H. A. Erlich.** 1989. The polymerase chain reaction. Trends Genet. **5:**185–189.
39. **Zervos, A. S., J. Gyuris, and R. Brent.** 1993. Mxi1, a protein that specifically interacts with Max to bind Myc-Max recognition sites. Cell **72:**223–232.
40. **Zhang, S., M. J. Ruiz-Echevarria, Y. Quan, and S. W. Peltz.** 1995. Identification and characterization of a sequence motif involved in nonsense-mediated mRNA decay. Mol. Cell. Biol. **15:**2231–2244.
41. **Zuk, D., A. H. Brown, S. Liebman, and A. Jacobson.** Unpublished data.